THE EFFECTS OF TEMPERATURE AND RADIATION ON CURRENT INSTABILITIES CAUSED BY RECOMBINATION CENTERS IN SEMICONDUCTORS

A Thesis

Submitted to the

Faculty of Graduate Studies and Research

The University of Manitoba

In Partial Fulfillment

of the Requirements for the Degree of

Master of Science

by

ABDELRAHMAN R. ELSHARKAWI

October, 1971

ABSTRACT

The current-voltage (I-V) characteristics of n-GaAs containing Coulombic recombination centers as functions of temperature and impurity concentration have been derived, and the current instabilities in n-GaAs as functions of temperature have been experimentally studied. The results show that the threshold voltage for the onset of negative differential resistance decreases with increasing temperature, while the corresponding current is temperature independent. The temperature dependence of the threshold voltage is in reasonable agreement with the theory.

The effects of gamma irradiation on the I-V characteristics and current oscillations have also been investigated. The results show that the threshold voltage decreases and the corresponding threshold current increases with increasing integrated radiation dose.

TABLE OF CONTENTS

LIST OF FIGURES

ACKNOWLEDGEMENTS

The author wishes to express his sincere thanks to Dr. K. C. Kao for his valuable guidance and encouragement during the course of this work, and to the Defence Research Board of Canada for financially supporting this work under Grant Number 5501-65 through Dr. K. C. Kao.

The author wishes also to thank Mr. R. J. Sill of the Materials Research Laboratories for his great assistance in the experiments and to the staff and colleagues in the Electrical Engineering Department for their help and cooperation.

CHAPTER 1

INTRODUCTION

During the 1950's and the early 1960's Ridley and Watkins (1961), Bonch-Bruevich (1965) and many other investigators (Bibliography on Gunn Effects, 1968 and 1969, by Gaylord, Shah, and Rabson), have discussed the possibility of obtaining a negative differential conductivity and so producing current instabilities in a semiconducting crystal subjected to a high electric field. This subject has been extensively studied by many investigators since the discovery of the Gunn effect in 1963. It is now known that a negative differential conductivity may arise in a semiconducting material due to several possible mechanisms, and some of these are listed below.

1. The field-enhanced interband transfer mechanism (FEIT).

   The carrier transfer from a valley of low energy with high carrier mobility to a valley of higher energy with low carrier mobility in the conduction band. This mechanism is generally referred to as the field-enhanced interband transfer mechanism, which was first suggested by Ridley and Watkins (1961) and Hilsum (1962), and later observed and discussed by Gunn (1963, 1964), Foyt (1965), Butcher (1967) and many other investigators.

2. The field-enhanced trapping mechanism (FET).

This mechanism is based on the field dependence of the capture rate of charge carriers by coulomb recombination centers (Ridley and Watkins, 1961; Bonch-Bruevich, 1965). When an applied electric field is high enough to produce hot carriers to surmount the surrounding barriers, the carriers are trapped and then the number of free carriers decreases with increasing applied field.

3. Negative differential resistance caused by double injection of carriers.

Double injection can be produced by two ohmic contacts, one at the cathode to inject electrons and the other at the anode to inject holes. The current-controlled negative resistance is due to the fact that the free carrier lifetime increases with increasing injection level. This is not the only cause for the occurrence of n.d.r. If there is only one ohmic contact to provide one type of carrier, the other type of carrier can be produced either by impact ionization or by field emission at high fields (Ando, 1963 and 1964).

4. Negative differential resistance due to impact ionization of impurities with the application of a magnetic field (McWhorter and Rediker, 1960; Phelan and Love, 1964)

For highly doped semiconductor, the impurity levels merge in the conduction band. The magnetic field

will cause a separation of these levels from the conduction band. If such a separation is larger than $k_B T_o$ (where k_B is the Boltzman constant, and T_o is the lattice temperature), freezeout occurs and electrons will be bound to impurity states resulting in an increase of the bulk resistivity. Upon the application of sufficiently high electric field, the electrons in the conduction band can acquire enough energy to impact ionize the impurities causing a lowering of the resistivity. If the resistance drops rapidly enough with increasing current, a negative differential resistance characteristic can be observed.

5. Negative differential resistance due to electron-phonon interaction.

Because of the energy transfer from electrons to acoustic waves travelling in the direction of drifting electrons, the current-voltage characteristics are non-ohmic (Huston, McFee and White, 1961; Gruvich, Kagan and Laichtman, 1964; Yamamoto, 1966). The negative differential resistance which leads to current oscillation is due to the formation of shock waves in a crystal on the abrupt application of a voltage pulse. These waves travel back and forth across the crystal. Of course, this type of oscillation would damp out after several periods of oscillation. However, continuous oscillations could occur in a crystal with two resis-

tivity regions, such as by illuminating part of the crystal.

Experimental work carried out by the aforementioned investigators and others supported these proposed mechanisms. But as far as theoretical investigations are concerned, no great deal has been done to describe quantitatively the observed phenomena, except for the first mechanism. The present work will be confined to the second mechanism, namely, the field-enhanced trapping, following the model proposed by Ridley and Watkins (1961), but in more detailed form. The problem will be treated by obtaining the current-voltage relationship from the general transport equation.

Chapter 2 presents a brief review of the previous theoretical work on the FET mechanism and some of the experimental results obtained by several investigators. In Chapter 3 a simplified mathematical theory is presented and the computation of the electron distribution function and the current-voltage characteristics are also given. The experimental techniques are given in Chapter 4 and the experimental results in Chapter 5. The theoretical and experimental results are discussed in Chapter 6.

CHAPTER 2

REVIEW OF PREVIOUS WORK

2.1 Theoretical Models

Ridley (1961b) proposed a model for the field-enhanced trapping mechanism and the condition for achieving a negative differential resistance (n.d.r.) region in the current-voltage characteristic of a semiconducting material. To achieve such a condition, the rate of capturing carriers by repulsive coulomb centers must increase as the applied electric field increases, since this will alter the equilibrium distribution of electrons over the various energy states in a semiconductor. In particular, a decrease in carrier density will lead to the occurrence of an n.d.r. region in the current-voltage characteristic. All the various energy states can be roughly divided into two main groups on the basis of the different mobilities of the electrons occupying them. By labelling the two groups "a" and "b", the current density is given by

$$J = e(n_a\mu_a + n_b\mu_b)F \qquad [2.1]$$

where n_a and n_b are the electron densities, and μ_a and μ_b their mobilities, in groups "a" and "b", respectively. The

action of the field will be:

1. To alter the electron mobilities.

2. To raise their energies, resulting in a change of the population among the different conduction groups.

The condition for the occurrence of the negative differential resistance is that $\frac{dJ}{dF}$ must be negative. Thus, by assuming $n_a + n_b$ = constant and letting $f = \frac{n_b}{n_a}$, we have

$$\left(\frac{\mu_a - \mu_b}{\mu_a + f\mu_b}\right)\left(-\frac{F}{n_a}\frac{dn_a}{dF}\right) - \frac{F}{\mu_a + f\mu_b}\left(\frac{d\mu_a}{dF} + f\frac{d\mu_b}{dF}\right) > 1 \qquad [2.2]$$

If the effect of the field is to increase the population in group "b", then it is essential that $\mu_b < \mu_a$ in order to satisfy the inequality given in Eqn. [2.2]. For the ideal case of localized states (trap centers), in which $\mu_b = 0$, only the group "a" represents the electrons in the conduction band. The population in group "a" is governed by the rates of transition associated with the impurity levels and the impact ionization. If we assume the change in the conduction electrons density to be Δn, and the mobility to be proportional to F^p, where p is a constant depending upon scattering mechanism, then the condition for the occurrence of n.d.r. becomes

$$\frac{F}{n_a}\frac{d\Delta n}{dF} - p > 1 \qquad [2.3]$$

The most favourable case is that when optical phonon scattering is dominant, where the factor p approaches -1. However, Bonch-Bruevich (1964, 1965) treated the problem for the case of acoustical phonons and concluded that such a scattering mechanism may give rise to an n.d.r. region.

By considering the polar optical scattering to be dominant in n-type GaAs, Law and Kao (1970) approximated the carrier distribution function by a Maxwellian function and the scattering effect by a relaxation time. Based on these assumptions, n.d.r. regions appeared in the derived current-voltage characteristics for different doping concentrations.

2.2 Experimental Work

So far, experimental investigation has been conducted on Ge, Si, and some III-V compounds, mainly GaAs and InSb. Almost all the current-voltage characteristics obtained showed an unstable region in which self-oscillations occur. Stable regions with n.d.r. have also been observed. The difference between the two regions might be thought of as due to the different origins of n.d.r.

The I-V curves can be divided into two groups characterized by their shapes (Pamplin, 1970). The first is the S-shaped curve characteristic of the current controlled negative differential resistance, as shown in Fig. 2.1. The second is the N-shaped curve characteristic of the voltage controlled n.d.r., as shown in Fig. 2.2.

For a sample exhibiting an S-shaped curve, the current has to be supplied to the sample from a constant current source. Initially, the I-V curve obeys Ohm's law, but soon the average electric field falls below the expected value until a critical point on the curve (J_{th}) at which the n.d.r. region starts. In this region, the sample is capable of conducting the current at a lower voltage. This region can be divided into two subregions; high and low current densities. Most of the current is carried in a filament-like path through the sample which is the high current density region, and the rest of the sample returns to the ohmic region of the I-V characteristic.

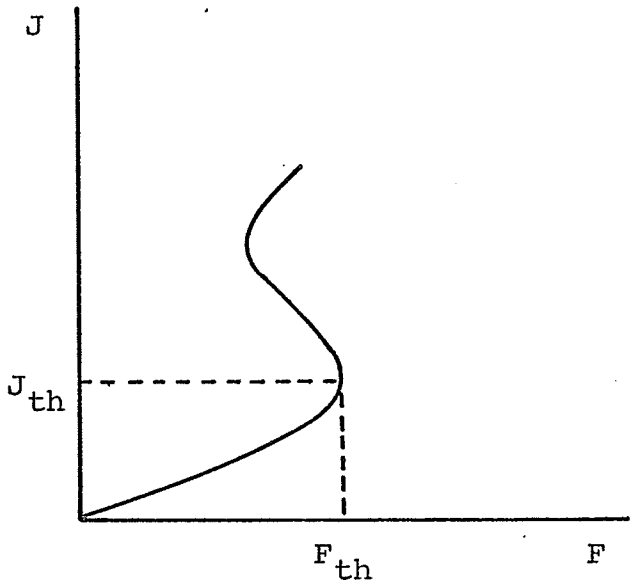

Fig. 2.1. S-shaped curve characteristic.

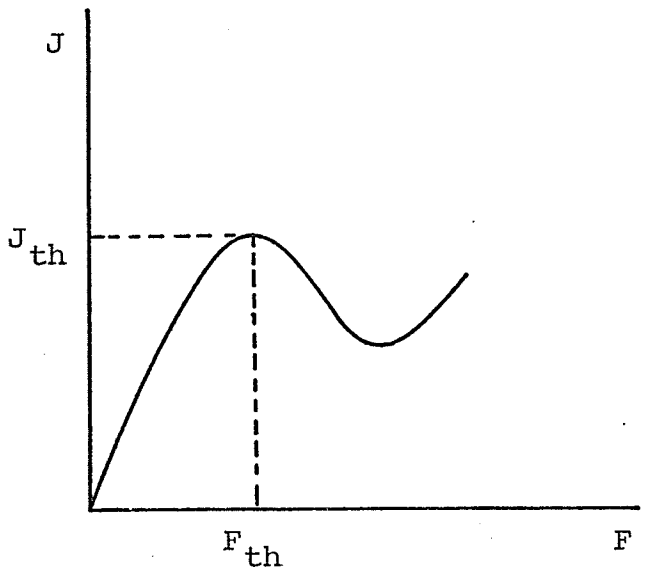

Fig. 2.2. N-shaped curve characteristic.

In a sample exhibiting an N-shaped curve the n.d.r. is a voltage controlled type. As the applied voltage increases, the I-V characteristic initially follows Ohm's law in a manner similar to that of the S-shaped type, but when the applied field reaches a critical point (F_{th}) the current starts to fall and the n.d.r. region begins. The threshold field can thus be defined as the average applied field which causes n.d.r. to occur. The threshold field, frequency, and amplitude of current oscillations are dependent on material, carrier concentration, temperature, hydrostatic pressure, and photo-illuminance.

Current oscillations due to recombination and trapping effects have been observed in Ge, Si and GaAs samples and effects of the afore-mentioned factors have been reported by many investigators. The important results are summarized next.

2.2.1 Effects of Temperature

Dorman (1967) has observed two different types of current waveform depending on temperature and light intensity. The first type has a frequency of approximately 6 kc/s, while the second approximately 1 kc/s. The waveform is similar in shape to that generated due to the Gunn effect (Foyt, 1965). Dorman also found that, below a certain critical temperature, only the low frequency oscillations could be observed. However, if the sample is warmer than this critical temperature, both high and low frequency oscillations could be obtained

depending on the light intensity. Bohm (1966) observed oscillations associated with an S-type n.d.r. in semi-insulator GaAs samples with a frequency of approximately 22 kc/s. The threshold current (J_{th}) for such oscillations is temperature dependent (inversely proportional). Thus, the longer the pulses are applied to the sample the smaller the threshold value for n.d.r.

Shirafuji (1969) observed the N-type n.d.r. in high resistivity GaAs samples. He found that the threshold field (F_{th}) for the oscillations decreases with decreasing temperature, as shown in Fig. 2.3. Kurova and Kalashnikov (1964) found that in n-type germanium the oscillation period decreases exponentially with the increase of temperature, as shown in Fig. 2.4. The above results indicate that the temperature plays a main role in the nature of oscillations and consequently in the mechanism responsible for such oscillations.

2.2.2 Effects of Carrier Concentrations

Moore *et al.* (1965) have reported that in high purity Co-compensated n-type silicon ranging in resistivity from 1.8 to 140 ohm-cm current oscillations occur at a field of 3 kv/cm, with a frequency from a few kilocycles to about 2 megacycles per second. The oscillations generally have large amplitude, and are seldom sinusoidal and very sensitive to light illumination. The oscillations in silicon lightly compensated with Au frequently appear much

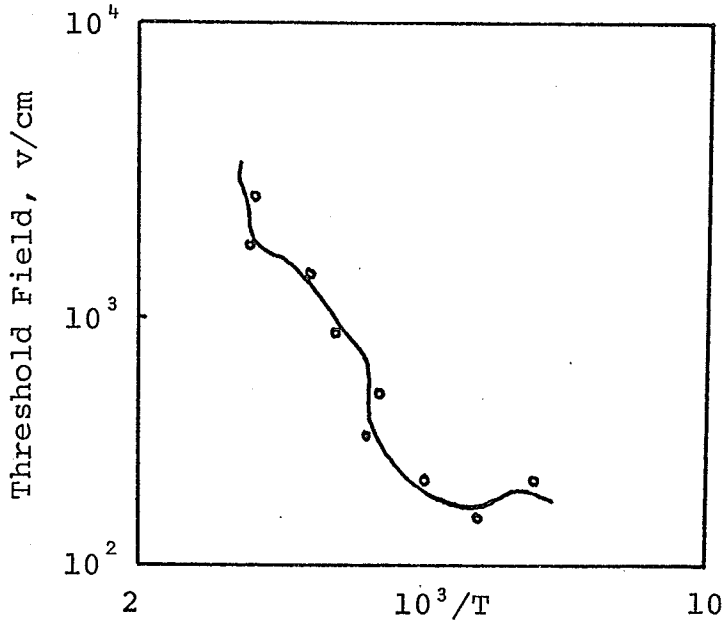

Fig. 2.3. Temperature dependence of threshold field. (After Shirafuji, 1969).

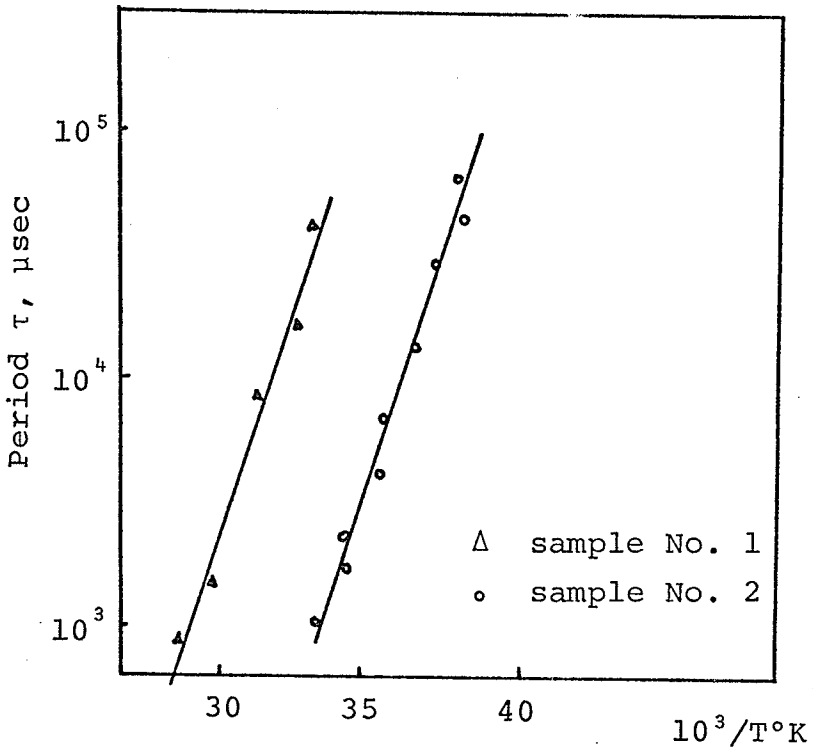

Fig. 2.4. Temperature dependence of oscillation period. (After Kurora and Kalashnikov, 1964).

like those in Co-compensated silicon, but in silicon samples heavily compensated with Au ($\sim 10^5$ ohm-cm compensated resistivity) the oscillations have a quite different feature. At the threshold field, the oscillations are generally nearly sinusoidal with the frequencies ranging from 3 Mc/s to greater than 60 Mc/s depending on the gold concentration (Fig. 2.5). These oscillations are not so sensitive to light illumination as those in Co-compensated silicon. In his experiments, Shirafuji (1969) found that the frequency of oscillations is strongly dependent on carrier concentration, which is a distinctive feature of the oscillations due to the field-enhanced trapping mechanism. The dependence of the n-F curve on electron concentration and temperature is given in Fig. 2.6.

2.2.3 Effects of the Applied Electric Field

Tokumaru (1967) observed high frequency ($\sim$Mc/s) and low frequency ($\sim$kc/s) current oscillations in photoexcited long n-type GaAs, oxygen doped to a concentration of about $10^{13}/cm^3$. The threshold field for the high frequency oscillations is about 4×10^3 v/cm and for low frequency oscillations, about 1.5×10^3 v/cm. At an average applied field greater than 4 kv/cm, high frequency oscillations occur first and continue for a while, then low frequency oscillations take place. For the high frequency oscillations, the dependence of frequency on the illumination intensity or applied voltage is negligible as compared with that for low

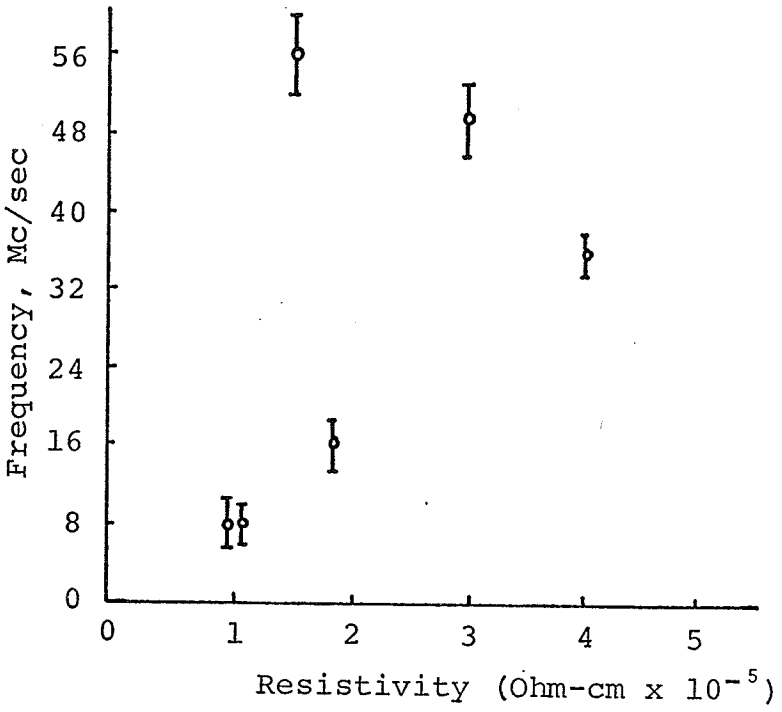

Fig. 2.5. Dependence of oscillation frequency on electron concentration. (After Moore *et al.*, 1965, with n-type Si sample).

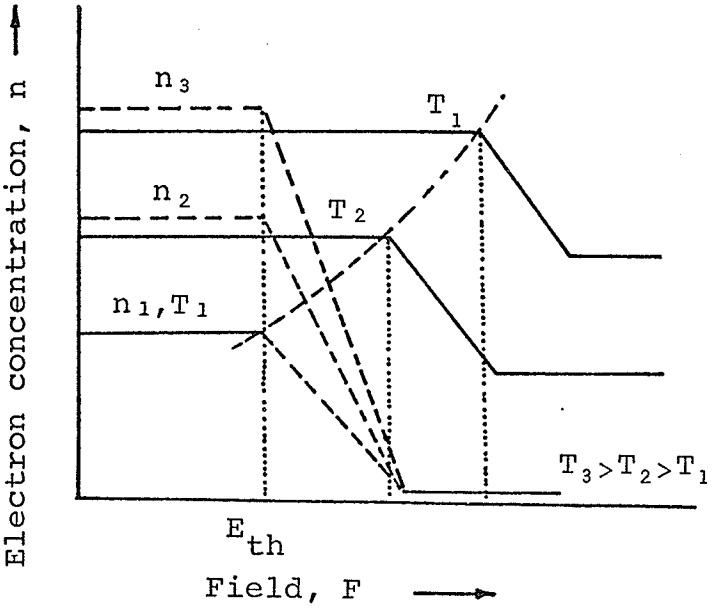

Fig. 2.6. Temperature (full lines) and electron concentration (dashed) dependence of the n-F curve. (After Shirafuji, 1969).

frequency oscillations. The duration of the high frequency oscillations decreases as the applied voltage is raised. Schematic current-voltage and current-time characteristics are given in Fig. 2.7 and Fig. 2.8. A similar phenomenon has also been observed by Day (1965) in high resistivity GaAs samples under different bias conditions. The samples are 3×10^3 ohm-cm in resistivity and 10^{-2} cm thick. He observed the high frequency oscillations ($\sim$1 Gc/s) under pulsed bias and the low frequency oscillations under d.c. bias.

Ridley and Wisbey (1969) have observed current oscillations in germanium samples at fields above 120 v/cm without light excitation. The frequencies of oscillations are 6 - 30 cpm and their amplitudes are small, except in some cases when the samples are biased at a field close to the threshold.

2.2.4 Effects of Light Illumination

Shirafuji (1969) found that at room temperature the current oscillations occur even in the dark. When the temperature decreases the dark current oscillations stop at a certain critical temperature, but application of light illumination generates them again. Dorman (1968) observed two different waveforms with different frequencies depending on the light intensity. An increase in light intensity causes a switch from higher to lower frequency waveforms. Current waveforms under different illumination conditions are given in Fig. 2.9. Moore *et al.* (1965) found that if a

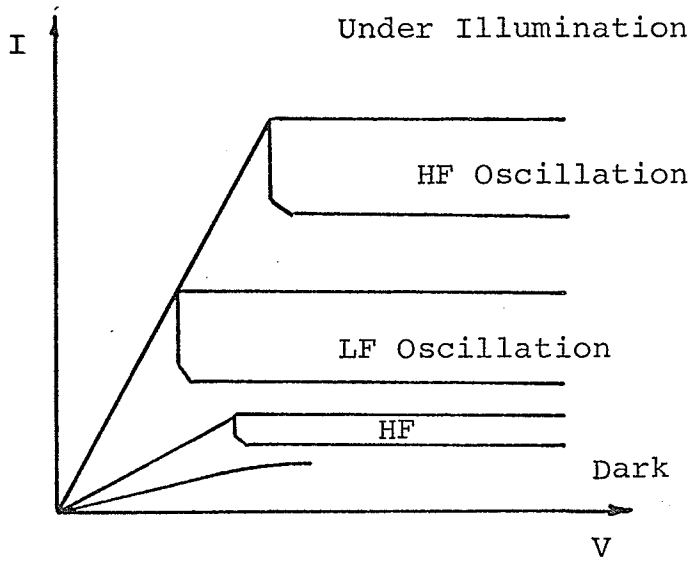

Fig. 2.7. Change of oscillation frequency with bias field. (After Tokumaru, 1969).

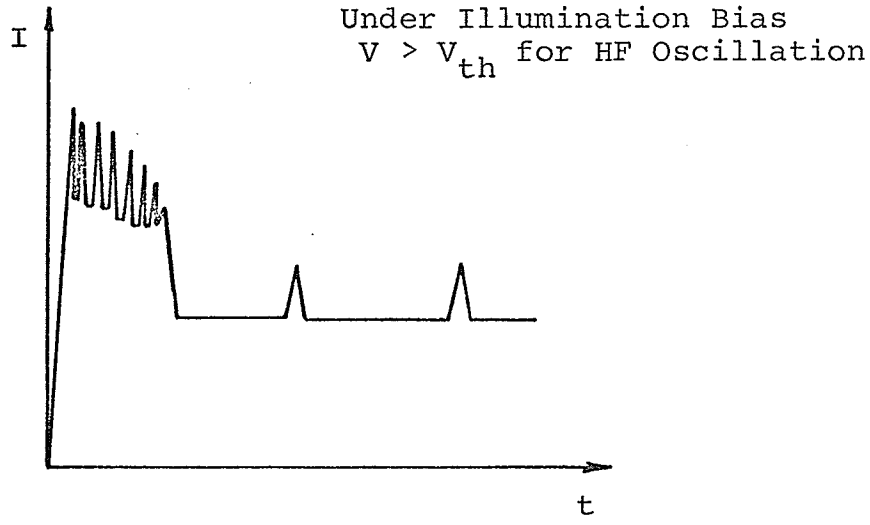

Fig. 2.8. Schematic current-time characteristic. (After Tokumaru, 1969).

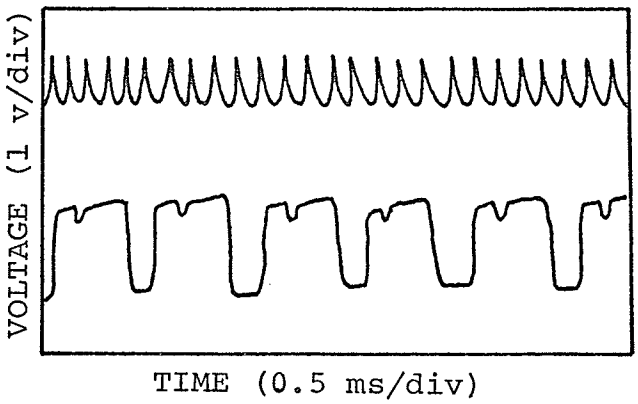

Fig. 2.9. Change of frequency with illumination. (After Dorman, 1969).

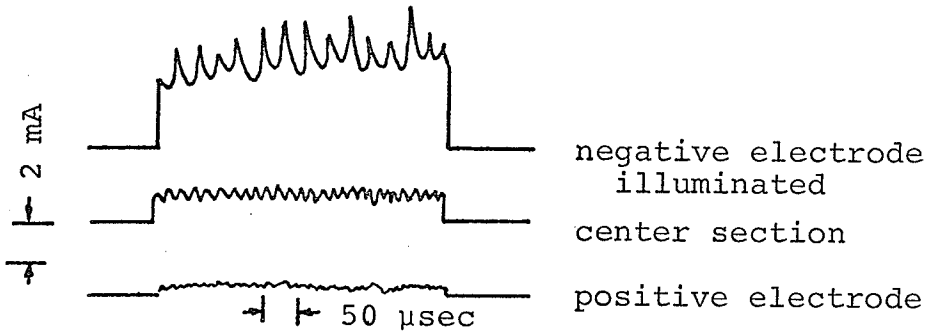

a) Polarity arbitrarily chosen

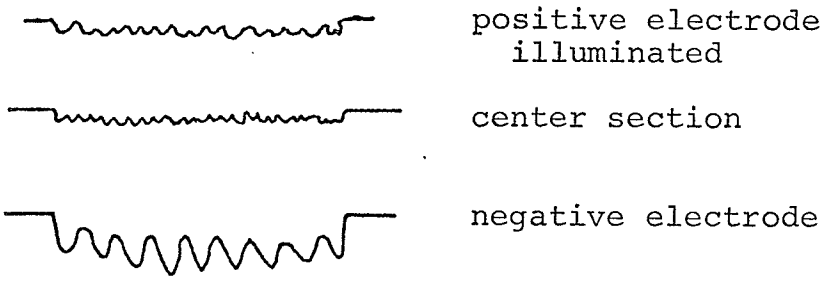

b) Polarity reversed from (a)

Fig. 2.10. Change of amplitude with illumination. (After Moore *et al.*, 1965).

fine beam of white light is incident on the sample, the amplitude of the oscillations is enhanced as the beam moves from anode to cathode, as illustrated in Fig. 2.10. Negative resistance regions and current oscillations in semiconducting samples have been observed by many other investigators, such as Ridley and Pratt (1963, 1964), Sugiyama (1967), Kikuchi (1967) and Matsumo (1968).

CHAPTER 3

THEORETICAL ANALYSIS

For an appropriate theoretical treatment of the problem under consideration, it would be desirable to first calculate the electronic momentum distribution in the presence of a homogeneous external field, and then to derive the current voltage characteristics. It is also essential to examine the factors affecting the conduction electrons density. Since we are concerned with the recombination centers in III-V compounds, it is important to know the origin of such centers so as to evaluate their physical criteria. In the following, we shall begin with a discussion of the formation of such centers.

3.1 The Formation of Coulombic Recombination Centers in Polar Crystals

In polar semiconductors, such as GaAs, any deviation from the stoichiometric composition (e.g. the imperfection due to impurities or lattice defects) would introduce trapping centers which are known to have considerable influence on many physical properties.

If an excess neutral impurity atom takes the normal positive ion position, there will be a lack of host atoms

to fill in all the positions reserved for negative ions, and hence a negative ion vacancy is created. This vacancy which is surrounded by positive ions tends to trap an electron, and it is normally referred to as the recombination center. If a neutral excess impurity atom occupies a negative ion position, a positive ion vacancy is produced. This vacancy, which is surrounded by negative ions will repel an electron, but trap a hole.

In n-type GaAs, oxygen atoms and other impurities generally attract minority carriers and possess a large capturing cross-section for them. After the capture of holes they form recombination centers which will be repulsive to the majority carriers (electrons) due to the polarization of the neighbouring atoms. The centers are located in the forbidden gap, and they behave as if the trapping center is surrounded by a potential barrier of height ϕ above the edge of the conduction band, and then droops down to a potential well, as shown in Fig. 3.1. The value of ϕ depends mainly on the electro-negativity of the center, and consequently on the doping material or impurity. Also, it depends on the distribution of the surrounding electrons and hence on the lattice temperature and the applied electric field. Barriers of up to 0.2 ev have been observed in germanium containing copper, nickel or gold by Battey and Baum (1955), Shulman and Wyluda (1956) and Johnston and Levinstein (1960). The temperature dependence of ϕ is not yet known.

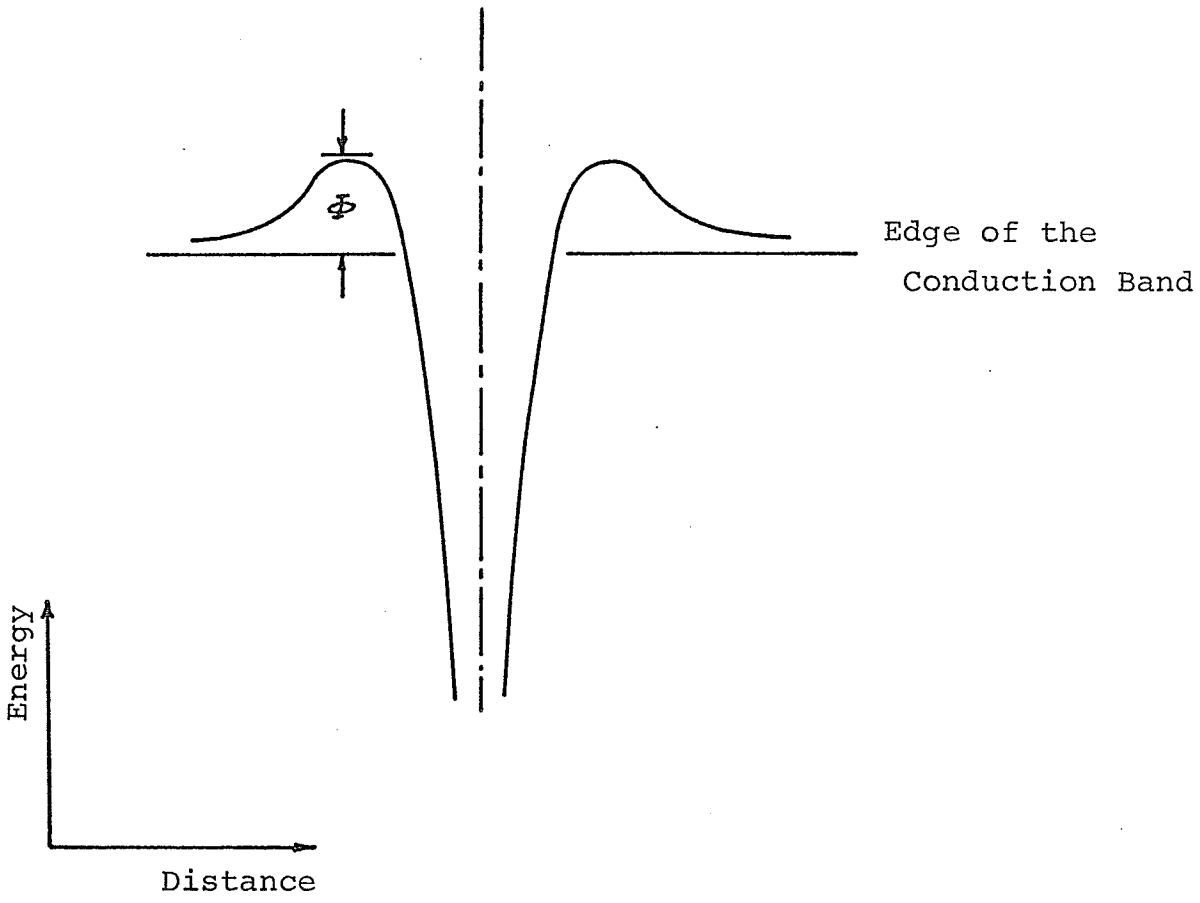

Fig. 3.1. Diagram of repulsive Coulomb center.

3.2 Charge Carrier Density Distribution

It is generally assumed that the presence of the recombination centers throughout the crystal will not change the form of the carrier distribution function when the carriers are ejected thermally into the conduction band after temporary storage in the centers due to the trapping action. However, the conduction carriers density will depend on the applied electric field and temperature.

If n is the density of the conduction electrons and N_0 the density of the unfilled recombination centers, then the carrier capture rate is given by

$$\left.\frac{\partial n}{\partial t}\right|_{cap} = - C_n n N_0 \qquad [3.1]$$

where C_n is the capture coefficient.

On the other hand, if g is the thermal ionization rate from these centers and N_- is the density of the filled recombination centers, then the rate of increase of conduction electrons due to thermal generation, is given by

$$\left.\frac{\partial n}{\partial t}\right|_{gen} = g N_- \qquad [3.2]$$

As will be seen later, the value of C_n depends on both the applied electric field and lattice temperature, but we shall assume that the thermal generation rate depends only on the lattice temperature and is not appreciably

affected by the field. At the steady state, both rates are equal and therefore we have

$$C_n n N_0 = g N_- \qquad [3.3]$$

Hence

$$n = \frac{g}{C_n} \frac{N_-}{N_0}$$

The oxygen atoms in n-GaAs introduce a shallow donor level close to the conduction band edge, which is assumed to be fully ionized at all temperatures, as well as a deep trapping level. Denoting the former by N_d and the latter by N_t , then for the charge neutrality condition we must have

$$N_0 = N_t - (N_d - n) \qquad [3.4]$$

and

$$N_- = N_d - n \qquad [3.5]$$

Substituting Eqns. [3.4] and [3.5] in Eqn. [3.3] we obtain

$$n = \tfrac{1}{2}\{(N_d - N_t - \frac{g}{C_n}) - [(N_d - N_t - \frac{g}{C_n})^2 + 4 \frac{g}{C_n} N_d]^{\frac{1}{2}}\} \qquad [3.6]$$

This equation shows the dependence of the free charge density on the lattice temperature, as well as on the applied electric field, through the dependence of C_n and g on these two

parameters.

The capture of an electron by a negatively charged impurity center in a semiconductor is strongly influenced by the presence of the potential barrier surrounding it. In order to be captured, an electron has to surmount this barrier. Thus, the lower the temperature, the smaller will be the thermal energy of the electrons and hence the greater will be the effect of the barrier. It is therefore obvious that the capture rate depends on both the applied electric field and the lattice temperature, since they tend to provide energy to the electrons.

The ionization of impurity atoms depends on the properties of such atoms and on the available thermal energy or the lattice temperature. Based on the law of mass action and Fermi statistics it can be shown (Spenke, 1958) that the generation rate is

$$g = \sigma_+ \, v_{th} \, \frac{N_c}{2} \exp\left(-\frac{E_t}{k_B T_o}\right) \qquad [3.7]$$

where k_B is the Boltzmann constant, T_o is the lattice temperature, $v_{th} = \left(\frac{3k_B T_o}{m^*}\right)^{\frac{1}{2}}$ is the mean thermal velocity of the electrons where m* is the effective electron mass, $N_c = 2\left(2\pi m^* \frac{k_B T_o}{h^2}\right)^{\frac{3}{2}}$ is the effective density of states in the conduction band where h is Plank's constant, E_t is the impurity trapping level measured from the conduction band edge, and σ_+ is the effective (geometric) cross-section of

the impurity atom which may be taken to be $(3 \times 10^{-8})^2$ cm based on quite arbitrary assumptions (Spenke, 1958), and it is assumed to be temperature independent. Hence, we have

$$g = 10^{-15} \left(\frac{54\pi}{h^2}\right)^{\frac{3}{2}} m^* (k_B T_o)^2 \exp\left(\frac{-E_t}{k_B T_o}\right) \qquad [3.8]$$

3.3 Boltzmann Transport Equation

The carrier distribution function (f) is generally given by the Boltzmann transport equation

$$\frac{\partial f}{\partial t} = -\left[\frac{\partial f}{\partial t}\right]_{scat} + \hbar^{-1} F \cdot \nabla_k f + v \cdot \nabla_r f \qquad [3.9]$$

where

$\hbar$ = Plank's constant divided by 2π

F = the external applied force

v = the electron velocity

On the right hand side of the equation, the last term can be ignored if the material is spatially homogeneous, and the second term represents the effect of external forces. In the present investigation, these external forces would be the electric field. The term $\left[\frac{\partial f}{\partial t}\right]_{scat}$ can be written as

$$\left[\frac{\partial f}{\partial t}\right]_{scat} = \left(\frac{\partial f}{\partial t}\right)_{e\text{-}e} + \left(\frac{\partial f}{\partial t}\right)_{scat} \qquad [3.10]$$

where

$\left(\frac{\partial f}{\partial t}\right)_{e\text{-}e}$ is the effect due to carrier-carrier scattering, and

$\left(\frac{\partial f}{\partial t}\right)_{scat}$ is the effect due to other types of scattering.

Of the scattering mechanisms that determine the

transport properties of n-type GaAs, the most important one at temperatures higher than 20°C is the polar interaction (Eherenriech, 1960). However, a distribution function which ignores electron-electron scattering almost certainly does not lead to a stable region of negative resistance (Adawi, 1960). In order to examine the effect of $(\frac{\partial f}{\partial t})_{e-e}$ on the distribution function, we shall compare the rates of energy loss of the high-energy electrons to the other electrons with that to the lattice vibrations.

The rate of loss of energy by electron-electron scattering is given by (Straton, 1958)

$$(\frac{dE}{dt})_{e-e} \sim \frac{4\pi n e^{*4}}{(2m^*E)^{\frac{1}{2}}} \qquad [3.11]$$

where

e^* = the effective electronic charge which takes account of the dielectric polarization of the medium and $(\frac{e^*}{e})^2 = \frac{1}{k}$ where k is the dielectric constant.

The corresponding rate of energy loss for collision of electrons with the polar modes is given by (Straton, 1958)

$$(\frac{dE}{dt})_{e-p} \sim \frac{eF_o \bar{h}\omega_l}{(2m^*E)^{\frac{1}{2}}} \ln(\frac{DE}{\bar{h}\omega_l}) \qquad [3.12]$$

where

ω_l = the angular frequency of longitudinal optical

phonons

F_o = a quantity with the dimensions of an electric field defined by

$$F_o = \frac{m^* e \omega_l}{\hbar} \left(\frac{1}{k_\infty} - \frac{1}{k_0}\right) \qquad [3.13]$$

where k_0 and k_∞ are the static and high frequency dielectric constants, respectively

$\hbar\omega_l$ = phonon energy (constant)

D = a pure number defined by

$$\ln D = \ln 4 - \ln c \simeq 0.8091$$

where c is Euler's constant.

The electron-electron scattering becomes dominant if $\left(\frac{dE}{dt}\right)_{e-e} >> \left(\frac{dE}{dt}\right)_{e-p}$. This inequality is controlled by the electron density n which varies with the carrier energy. The two rates become equal at an electron density given by (neglecting the logarithmic term)

$$n_o \simeq \frac{eF_o \hbar\omega_l}{4\pi e^{*4}} \qquad [3.14]$$

with the condition $k_B T_o >> \hbar\omega_l$. Above this critical electron density, the electron-electron scattering is sufficiently frequent to enforce a Maxwellian distribution characterized by an electron temperature T_e. The value of

n_o has been calculated for different materials by several investigators (Yamashita, 1960; Adawi, 1960; Oliver, 1962). Using $F_o = 4.62 \times 10^3$ v/cm, $\hbar\omega_l/k = 410°K$, and $k = 13$, Oliver has calculated n_o for GaAs to be 4.3×10^{10} cm^{-3}. Whatever the mechanism of energy loss, the density of electrons in most samples used for the investigation in this field to date exceeds the critical value n_o, and it is therefore legitimate to use the concept of electron temperature rather than electron density to discuss the experimental results.

3.4 The Concept of Electron Temperature

Electron temperature for carriers is the measure of their average energy (Frölich, 1956). When the density of electrons is high, the rate of energy exchange between electrons through mutual collisions is large compared with the rate of energy exchange between electrons and lattice vibrations. At the steady state, the average energy loss in a collision must be equal to the average gain from the field between collisions. If the rate, at which electrons gain energy from the field, exceeds the rate of loss by collisions; the mean electron energy increases and the mobility changes. Under such a condition it may be assumed that the electrons are in thermal equilibrium (though displaced in momentum space) at a temperature T_e which is higher than the lattice temperature T_o.

The assumption of an electron temperature T_e should be valid when the electron density is larger than its critical value n_o. In typical ionic crystals, it is usually assumed that the electrons interact with the optically active vibrations only when the former have the energy corresponding to approximately the same frequency ω_l (Frölich, 1954). If $k_B T_e << \hbar\omega_l$ most electrons cannot emit quanta. Scattering is then described as elastic in terms of a two-stage process, absorption and re-emmission of quanta $\hbar\omega_l$. Clearly, there is no energy transfer in such approximation. The only remaining energy transfer is then

either due to interaction with other electrons or due to interaction with acoustic waves, which is assumed to be very weak (Ehrenriech, 1960). Hence, for ionic crystals, the electron-electron scattering is important even at low electron densities.

In highly doped n-type GaAs the top of the impurity band merges into the conduction band. In this case, the impurity is responsible for both the spectrum and the scattering of charge carriers. Also, on raising the impurity concentration, the free carriers concentration is usually increased as well. Thus, the electron-electron scattering may become important. This leads, in particular, to the screening of the impurity fields by the free charges (Bonch-Bruevich, 1966).

3.5 The Distribution Function Based on Predominant Electron-electron Scattering

The carrier distribution function can be expanded in terms of Legendre polynomials (Law and Kao, 1969)

$$f(p) = \sum_{s=0}^{\infty} f_s(p)\, P_s(\cos\theta) \qquad [3.15]$$

where θ is the angle between the applied electric field and momentum . Due to the convergence of such polynomials the terms higher than the second can be neglected, and thus the distribution function can be approximated to

$$f(p) \simeq f_0(E) + f_1(E) \cos\theta \qquad [3.16]$$

where E and p are the electron energy and momentum, respectively. Frölich and Paranjape (1956) have shown that the rate of change of f(p) for optical modes can also be expanded in spherical harmonics, and therefore

$$\left(\frac{\partial f}{\partial t}\right) = \left(\frac{\partial f_0}{\partial t}\right) + \left(\frac{\partial f_1}{\partial t}\right) \cos\theta \qquad [3.17]$$

where

$$\left(\frac{\partial f_0}{\partial t}\right) = \frac{-eF_o N_q}{(2m^*E)^{\frac{1}{2}}}\left[\left\{f_0(E) - \exp\left(\frac{\hbar\omega_l}{k_B T_o}\right) f_0(E + \hbar\omega_l)\right\} \phi(E) + \left\{\exp\left(\frac{\hbar\omega_l}{k_B T_o}\right) f_0(E) - f_0(E - \hbar\omega_l)\right\}\phi(E - \hbar\omega_l)\right] \qquad [3.18]$$

and

$$\left(\frac{\partial f_1}{\partial t}\right) = -\frac{eF_o N_q}{(2m^*E)^{\frac{1}{2}}}\left[f_1(E)\phi(E) - \exp\left(\frac{\hbar\omega_l}{k_B T_o}\right) f_1(E + \hbar\omega_l)\right.$$

$$\times\left\{\frac{2E + \hbar\omega_l}{2(E(E + \hbar\omega_l))^{\frac{1}{2}}}\phi(E) - 1\right\} + f_1(E)\phi(E - \hbar\omega_l)\exp\left(\frac{\hbar\omega_l}{k_B T_o}\right)$$

$$\left. - f_1(E - \hbar\omega_l)\left\{\frac{2E - \hbar\omega_l}{2(E(E - \hbar\omega_l))^{\frac{1}{2}}}\phi(E - \hbar\omega_l) - 1\right\}\right] \qquad [3.19]$$

where

$$\phi(E) = \ln\frac{(E + \hbar\omega_l)^{\frac{1}{2}} + (E)^{\frac{1}{2}}}{(E + \hbar\omega_l)^{\frac{1}{2}} - (E)^{\frac{1}{2}}} = 2\sinh^{-1}\left(\frac{E}{\hbar\omega_l}\right)^{\frac{1}{2}} \qquad [3.20]$$

and N_q is the density of photons given by

$$N_q = \left[\exp\left(\frac{\hbar\omega_l}{k_B T_o}\right) - 1\right]^{-1} \qquad [3.21]$$

Therefore, we can write

$$f(p) = A\exp\left(\frac{|p - p_0|^2}{2mk_B T_e}\right) \qquad [3.22]$$

which is a displaced Maxwellian function, with a normalization constant "A" which can be determined from the normalization condition, so that

$$f_0(E) = A\exp\left(\frac{-E}{k_B T_e}\right) \qquad [3.23]$$

and

$$f_1(E) = A \frac{(2m^*E)^{\frac{1}{2}}}{m^* k_B T_e} p_o \exp\left(\frac{-E}{k_B T_e}\right) \qquad [3.24]$$

with the condition

$$\frac{p_o^2}{2m^* k_B T_e} << 1$$

The displacement p_o and the effective carrier temperature T_e can be determined from the condition for the conservation of energy

$$\int \{eF \left(\frac{\partial f}{\partial p}\right) + \left(\frac{\partial f}{\partial t}\right)_{scat}\} E \, d^3p = 0 \qquad [3.25]$$

and that for the conservation of momentum

$$\int \{eF \left(\frac{\partial f}{\partial p}\right) + \left(\frac{\partial f}{\partial t}\right)_{scat}\} p \, d^3p = 0 \qquad [3.26]$$

Substituting Eqns [3.23] and [3.24] into Eqn. [3.17] we get the form of the carrier distribution function in the momentum space. Using this function in solving Eqns. [3.25] and [3.26] we obtain (Paranjape, 1953)

$$\left(\frac{F}{F_o}\right)^2 = \left(\frac{2\pi}{3}\right) N_q^2 G_e^2 \exp G_e [\exp(G_o - G_e) - 1] K_0\left(\frac{G_e}{2}\right)$$

$$\times [\{\exp(G_o - G_e) - 1\} K_0\left(\frac{G_e}{2}\right) + \{\exp(G_o - G_e) + 1\}]$$

$$\times K_1\left(\frac{G_e}{2}\right) \qquad [3.27]$$

and

$$p_o^2 = \frac{(3m\hbar\omega_l)}{G_e} \left| 1 + \frac{\exp(G_o - G_e) + 1}{\exp(G_o - G_e) - 1} \frac{K_1(\frac{G_e}{2})}{K_0(\frac{G_e}{2})} \right|^{-1} \qquad [3.28]$$

where K_0 and K_1 are the modified Bessel functions of the zero and first order respectively, $G_o = \frac{\hbar\omega_l}{k_B T_o}$ and $G_e = \frac{\hbar\omega_l}{k_B T_e}$. Now we consider the following conditions:

1. At high lattice temperatures i.e. $G_o << 1$, Eqns. [3.27] and [3.28] can be simplified to

$$(\frac{F}{F_o})^2 = (\frac{8\pi}{3})(\frac{G_e}{G_o})(1 - \frac{G_e}{G_o}) \ln(\frac{D}{G_e}) \qquad [3.29]$$

$$p_o^2 = \frac{3}{4} m\hbar\omega_l G_o (1 - \frac{G_e}{G_o}) \ln(\frac{D}{G_e}) \qquad [3.30]$$

2. At low lattice temperatures i.e. $G_o >> 1$, but with high applied fields, Eqns. [3.27] and [3.28] approximately become

$$F^2 = F_o^2 (\frac{2}{3\pi}) G_e^2 \exp(-G_e) K_0(\frac{G_e}{2}) \times [K_0(\frac{G_e}{2}) + K_1(\frac{G_e}{2})] \qquad [3.31]$$

and

$$p_o^2 = 3m\hbar\omega_l [\{1 + \frac{K_1(\frac{G_e}{2})}{K_0(\frac{G_e}{2})}\} G_e]^{-1} \qquad [3.32]$$

This is equivalent to the condition on F as

$$F >> F_o \left(\frac{4G_o}{3}\right)^{\frac{1}{2}} \exp(-G_o) \qquad [3.33]$$

3. At low lattice temperatures with intermediate applied fields Eqns. [3.27] and [3.28] can be simplified to

$$F^2 = F_o^2 \frac{4}{3} G_e \exp(-2G_e) \qquad [3.34]$$

and

$$p_o^2 = \frac{3m\hbar\omega_l}{2G_e} \qquad [3.35]$$

This is equivalent to the condition on F as

$$F_o \left(\frac{4G_o}{3}\right)^{\frac{1}{2}} \exp(-G_o) << F << \frac{F_o}{5} \qquad [3.36]$$

3.6 The Distribution Function Based on Non-predominant Electron-electron Scattering

The distribution function must be determined from the steady state kinetic equation

$$\left(\frac{\partial f}{\partial t}\right)_i + \left(\frac{\partial f}{\partial t}\right)_F = 0 \qquad [3.37]$$

The first term on the left hand side represents the rate of change of the distribution function due to collision and the second term is the rate of change due to the applied field. From Eqn. [3.16] we have

$$\left(\frac{\partial f}{\partial t}\right)_F \simeq \left(\frac{\partial f_0}{\partial t}\right)_F + \left(\frac{\partial f_1}{\partial t}\right)_F \cos\theta \qquad [3.38]$$

Frölich (1947) calculated the values of the two terms on the right hand side. They are given by

$$\left(\frac{\partial f_0}{\partial t}\right)_F = \frac{2eF}{3} \frac{1}{(2m^*E)^{\frac{1}{2}}} \frac{d}{dE}(Ef_1) \qquad [3.39]$$

and

$$\left(\frac{\partial f_1}{\partial t}\right)_F = \frac{eF(2m^*E)^{\frac{1}{2}}}{m} \frac{\partial f_0}{\partial E} \qquad [3.40]$$

Based on the relaxation time approximation, $\left(\frac{\partial f}{\partial t}\right)_i$ for polar scattering is given by (Straton, 1958)

$$\left(\frac{\partial f}{\partial t}\right)_i = - \frac{f_1}{\tau_i(E)} \qquad [3.41]$$

with the relaxation time $\tau_i(E)$ for $E >> \hbar\omega_l$ given by

$$\frac{1}{\tau_i(E)} = eF_o \frac{(2N_q + 1)}{(2mE)^{\frac{1}{2}}} \qquad [3.42]$$

and the relaxation time for $E << h\omega_l$ by

$$\frac{1}{\tau_i(E)} = \frac{2eF_o N_q}{(2m\hbar\omega_l)^{\frac{1}{2}}} \qquad [3.43]$$

Hence, we obtain

$$f_1 = - \frac{eF_o(2m^*E)^{\frac{1}{2}}}{m} \tau_i(E) \frac{\partial f_0}{\partial E} \qquad [3.44]$$

For high energy electrons, we have

$$\left(\frac{\partial f_0}{\partial t}\right)_i = \frac{1}{(2m^*E)^{\frac{1}{2}}} \frac{d}{dE}[\delta_i\{f_0 + x_i \frac{df_0}{dE}\}] \qquad [3.45]$$

where

$$\delta_i = eF_o \hbar\omega_l \ln\left(\frac{4E}{\hbar\omega_l}\right) \qquad [3.46]$$

and

$$x_i = \hbar\omega_l (N_q + \tfrac{1}{2}) \qquad [3.47]$$

By solving Eqn. [3.45], we obtain

$$f_0 \sim \exp\left[-\int_E \frac{dE}{x_i + 2e^2F^2(2m^*E)^{\frac{1}{2}} \frac{E\tau_i}{3m\delta_i}}\right] \qquad [3.48]$$

or

$$f_0 \sim \exp\left[-\frac{1}{x_i}\int_E \frac{dE}{1 + 2E^2F^2/3F_o^2x_i^2\ln(\frac{4E}{\hbar\omega_l})}\right] \qquad [3.49]$$

and by simplifying the integration by considering $E \simeq k_BT_o$ in the logarithmic term, we obtain

$$f_0 = A\left[1 + \frac{2}{9\ln(\frac{4k_BT_o}{\hbar\omega_l})}(\frac{F}{F_o})^2(\frac{E}{k_BT_o})^2\right]\exp(-\frac{E}{k_BT_o}) \qquad [3.50]$$

Substitution of Eqn. [3.50] into Eqn. [3.44] gives

$$f_1 = A\frac{eF(2m^*E)^{\frac{1}{2}}}{mk_BT_o}\tau_i(E)\{[1 + \frac{2}{9\ln(\frac{4k_BT_o}{\hbar\omega_l})}(\frac{F}{F_o})^2(\frac{E}{k_BT_o})^2] \qquad [3.51]$$

$$- \frac{2k_BT_o}{E}[\frac{2}{9\ln(\frac{4k_BT_o}{\hbar\omega_l})}(\frac{F}{F_o})^2(\frac{E}{k_BT_o})^2]\exp(-\frac{F}{k_BT_o})$$

3.7 Calculation of the Capture Coefficient

The capture coefficient C_n is given by (Bonch-Bruevich, 1965)

$$C_n = \frac{\int f(\bar{k})\ \sigma(\bar{k})\ v(\bar{k})\ d^3k}{\int f(\bar{k})\ d^3k} \qquad [3.52]$$

where $v(\bar{k})$ is the carrier velocity, and $\sigma(\bar{k})$ is the capture cross-section. By assuming the energy band structure to be parabolic, the electron wave number is given by

$$k = \frac{(2m^*E)^{\frac{1}{2}}}{\hbar} \qquad [3.53]$$

The geometrical size of a center is not an adequate estimate for cross-section because the electron must not only come to the vicinity of the center, but it must also undergo the process of losing part of the energy. Therefore, the form of $\sigma(\bar{k})$ depends on the mechanism by which the energy removal takes place. In n-type GaAs, the energy can be transferred to the lattice, and used to create a phonon. Based on the time-dependent perturbation theory, the dominant energy dependent part of $\sigma(\bar{k})$ for such mechanism is given by (Law and Kao, 1969)

$$\sigma(\bar{k}) \sim [\exp\{\frac{h}{(2m^*E)^{\frac{1}{2}}}\ a_H\} - 1]^{-1} \qquad [3.54]$$

where a_H is the Bohr's radius and is given by

$$a_H = \frac{k\,\hbar^2}{m^* e^2 Z} \qquad [3.55]$$

where Z is the charge of the recombination center, and m* is the effective mass of the electron. Substitution of Eqns. [3.16], [3.53], and [3.54] into Eqn. [3.52] gives

$$C_n = \left(\frac{2}{m^*}\right)^{\frac{1}{2}} \frac{\int_0^\infty f_0 \;\; \sigma(E)\; E\; dE}{\int_0^\infty f_0 E^{\frac{1}{2}}\, dE} \qquad [3.56]$$

The values of C_n for the following conditions are:

1. At high temperatures, Eqn. [3.56] becomes

$$C_n = \left(\frac{2}{m^*}\right)^{\frac{1}{2}} \frac{\int_0^\infty \exp\left(-\frac{E}{k_B T_o}\right) \;\; \sigma(E)\; E\; dE}{\int_0^\infty \exp\left(\frac{-E}{k_B T_o}\right)\; E^{\frac{1}{2}}\, dE} \qquad [3.57]$$

with

$$F^2 = F_o^2 \left(\frac{8}{3\pi}\right)\left(\frac{G_e}{G_o}\right)\left(1 - \frac{G_e}{G_o}\right)\ln\left(\frac{D}{G_e}\right) \qquad [3.58]$$

2. At low temperatures, with high applied fields, C_n has the same expression as Eqn. [3.57], but with

$$F^2 = F_o^2 \left(\frac{2}{3\pi}\right) G_e^2 \exp(-G_e)\; K\left(\frac{G_e}{2}\right) \times \left[k_0\left(\frac{G_e}{2}\right) + k_1\left(\frac{G_e}{2}\right)\right] \qquad [3.59]$$

3. At low temperatures, with intermediate applied fields, C_n also is the same as Eqn. [3.57], but with

$$F^2 = F_o^2 \frac{4}{3} G_e \exp(-2G_e) \qquad [3.60]$$

4. At low temperatures, with low applied fields, Eqn. [3.56] becomes

$$C_n = \left(\frac{2}{m}\right)^{\frac{1}{2}} \frac{\int_0^\infty \exp\left(\frac{-E}{k_B T_o}\right) \sigma(E) \left[1 + \frac{2\left(\frac{F}{F_o}\right)^2}{9 \ln\left(\frac{4k_B T_o}{\hbar\omega_l}\right)} \left(\frac{E}{k_B T_o}\right)^2\right] E \, dE}{\int_0^\infty \left[1 + \frac{2\left(\frac{F}{F_o}\right)^2}{9 \ln\left(\frac{4k_B T_o}{\hbar\omega_l}\right)} \left(\frac{E}{k_B T_o}\right)^2\right] \exp\left(\frac{-E}{k_B T_o}\right) E^{\frac{1}{2}} \, dE} \qquad \ldots [3.61]$$

3.8 The Current-voltage Characteristics

The current density is given by the definition

$$\bar{J} = e\, n\, \frac{\int \bar{v}\, f\, d^3k}{\int f\, d^3k} \qquad [3.62]$$

where $\bar{v}$ is the velocity given by

$$\bar{v} = \frac{\hbar \bar{k}}{m} \qquad [3.63]$$

If the conduction band of n-GaAs is assumed to be parabolic, and the applied field is directed along the x-direction, then the current density is given by

$$J = \left(\frac{2}{9m}\right)^{\frac{1}{2}} e\, n\, \frac{\int_0^\infty f_1(E)\, E\, dE}{\int_0^\infty f_0(E)\, E^{\frac{1}{2}}\, dE} \qquad [3.64]$$

We solve Eqn. [3.64] for the following cases:

1. At high lattice temperatures, Eqn. [3.64] becomes

$$J = e\, n\, \frac{p_o}{m^*} \qquad [3.65]$$

with F and p given by Eqns. [3.29] and [3.30].

2. At low temperatures, with high applied fields, Eqn. [3.65] is also applied but with F and p_o given by Eqns. [3.31] and [3.32].

3. At low temperatures, with intermediate applied

fields Eqn. [3.65] is still applied, with the expressions for F and p_o given by Eqns. [3.34] and [3.35].

4. At low temperatures, with low applied fields, Eqn. [3.64] becomes

$$J = \frac{2e^2Fn}{3m} \frac{\int_0^\infty E^{\frac{3}{2}} \tau_i(E)\ \phi(E)\ \exp(\frac{-E}{k_B T_o})\ dE}{\int_0^\infty E^{\frac{1}{2}}\ \phi(E)\ \exp(\frac{-E}{k_B T_o})\ dE} \qquad [3.66]$$

with $\phi(E)$ and $\tau_i(E)$ given by Eqns. [3.20], [3.42], and [3.43].

3.9 Computed Results

The current-voltage characteristics have been computed using the following numerical values for n-GaAs

$$m^* = 0.072 \times (9.107 \times 10^{-28})\,g$$

$$e = 4.806 \times 10^{-10} \text{ e.s.u.}$$

$$k_B = 1.380 \times 10^{-16} \text{ erg-}^\circ K^{-1}$$

$$\hbar = 6.624 \times 10^{-27}/2\pi \text{ erg-sec}$$

$$\omega_l = 5.37 \times 10^{13} \text{ rad/sec}$$

$$k_\infty = 10.82$$

$$k_0 = 12.53$$

$$N_d - N_t = 10^{11} \text{ cm}^{-3}$$

$$N_d = 10^{16} \text{ cm}^{-3}$$

$$E_t = 0.1 \text{ ev}$$

and the results are shown in Fig. 3.2 for different temperatures. They are S-type curves as described in Chapter II. The curves are sensitive to changes of temperature. The higher the temperature, the lower is the value of the threshold field to start the n.d.r. region. The critical value of the current does not seem to be very sensitive to the lattice temperature. Another factor that affects the current-voltage characteristic is the impurity concentration. As the impurity increases the threshold field decreases. The trapping-center concentration depends on the impurity concentration, so an increase in the latter has the effect of increasing the capture rate, due to the increase in the

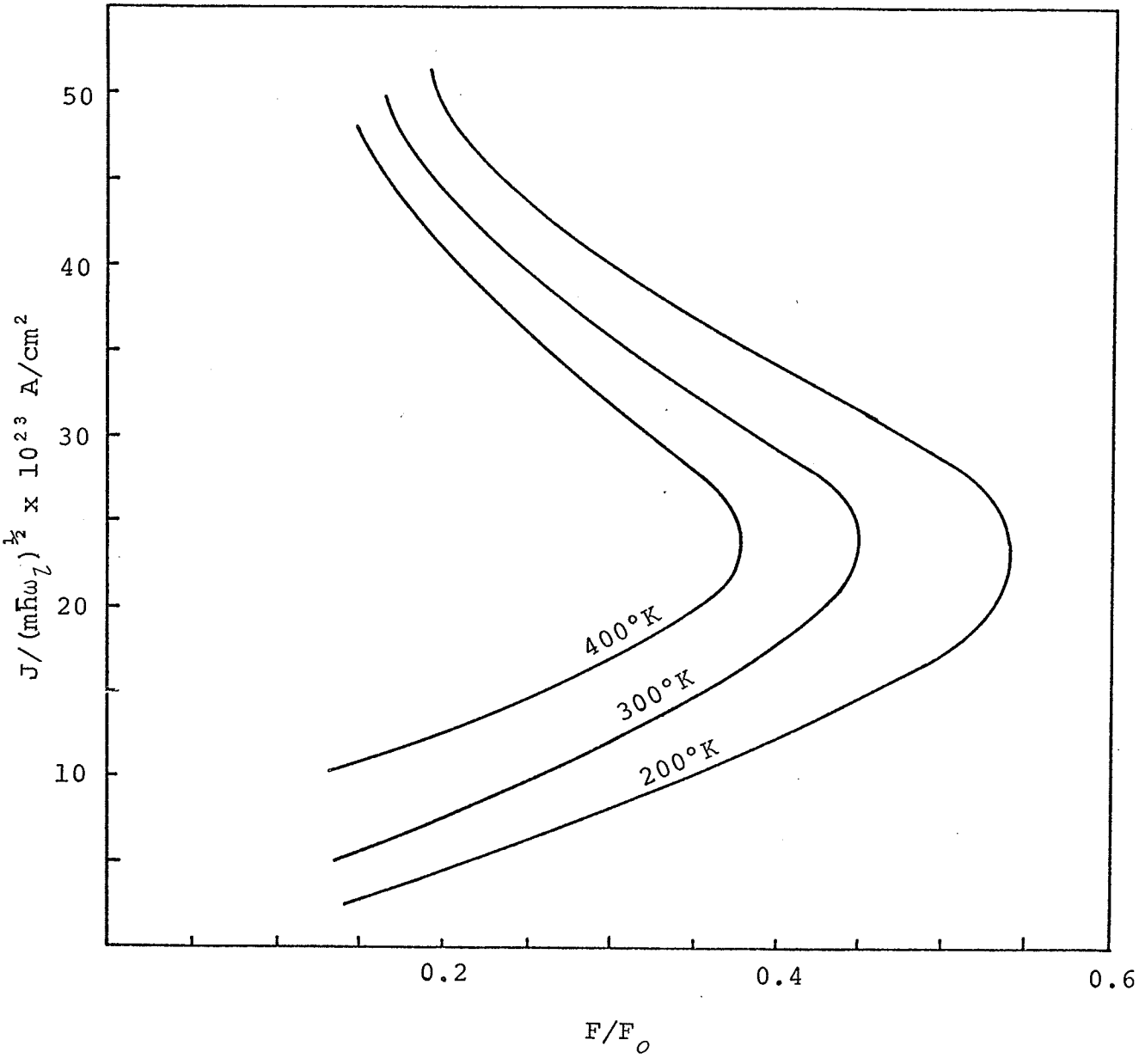

Fig. 3.2. Current-voltage characteristics

density of trapping centers, and thus lowering the critical value of the field.

Current controlled negative differential resistance of the S-type has been observed in n-GaAs by Mizushima *et al.* (1965), Bohm (1966), and Hughes (1968). This type of curves usually appears in thin samples with high electron concentration. Bohm (1966) used n-GaAs samples of 0.001 inch to 0.01 inch thick with resistivities of 10^6 - 10^8 ohm-cm and observed S-type n.d.r. The threshold current is temperature dependent (inversely proportional to temperature). The longer the pulses are applied, the smaller the value of the threshold field as a result of Joule heating. Illumination of the sample decreases the threshold field. This indicates that it depends greatly on the available charge carriers.

The high charge carrier concentration allows the use of a Maxwellian distribution for the distribution function with the proper effective carrier temperature. In this case the curve of electrical field F as a function of the electron temperature is a Van der Waals-type curve (Landau and Lifshitz, 1958). Thus a negative differential resistivity of the current controlled type is possible. Adawi (1961) has shown that in such case a voltage controlled n.d.r. is not possible.

CHAPTER 4

EXPERIMENTAL TECHNIQUES

The n-GaAs samples were obtained from Monsanto Chemical Company. The electrical and geometrical properties of these samples at 300°K are as follows:

Type: N

Dopant: Oxygen

Concentration: 1.4×10^{11} Atoms/cm^3

Resistivity: 1.4×10^3 ohm-cm

Mobility: 5400 cm^2 $volt^{-1}$ sec^{-1}

Orientation: 1-1-1

Thickness: 188 microns

Area: 0.75 x 0.75 mm^2

4.1 Preparation of the Samples

The most important step in preparation of the semiconducting n-GaAs samples is the fabrication of good ohmic contacts. These contacts must be nearly lossless and non-rectifying to avoid attenuation or distortion of the passing signals to the bulk of the semiconducting material. There are many known methods that can be used to produce such

contacts (Cunnell and Edmond, 1960; Dale and Turner, 1963; Cox and Strack, 1967). Different methods may have to be used for different samples depending on the electrical properties, geometrical properties, and experimental conditions. The method used here is the vacuum deposition method, similar to, but slightly different than, that used by Wu (1970). It should be mentioned that the surface cleanness plays a main role in the success of alloying a satisfactory contact on the semiconductor. The essential steps involved in the evaporated ohmic contacts on GaAs are:

a) Mechanically polish the sample surface with 5 micron size alumina powder, then 0.3 micron size to assure a high degree of smoothness. To facilitate the polishing job the sample was stuck onto a copper block with wax.

b) Remove the wax from the surface of the sample by rinsing in warm petroleum ether and then by rinsing in trichloroethylene. Wash with acetone to ensure the removal of any wax that can be left on the surface.

c) Etch for about a half minute in $Br_2 + CH_3OH$. Etching should be done in a fume cupboard since bromine is poisonous. After etching, the etchant remaining should be removed quickly by washing with deionized water. Care should be taken not to expose the sample to the atmosphere during the etching process to avoid

possible oxidation of the surface, since the bromine is an effective oxidizing agent.

d) Wash and then immerse in methanol until the vaccuum system is ready. Immersion in methanol will prevent oxidation.

e) Transfer the sample to the vacuum system (2×10^{-6} mm Hg pressure). A stainless steel mesh is used to produce 30 contacts per cm^2 on the surface of the sample, while the other surface is completely coated. It was found that direct heating of the sample under vacuum may help in assuring the production of the contact on the sample surface. Tin is first evaporated on the surface, then gold. After deposition the sample should be allowed to cool down in vacuum to prevent oxidation of the tin.

f) On heat treatment, the sample is heated for 5 minutes at a temperature of 450°C, then cooled to room temperature in N_2 atmosphere. The set-up for heat treatment of contacts is shown in Fig. 4.1.

g) Gold wire leads are connected to the ohmic contacts on both sides of the sample using the ultrasonic bonder.

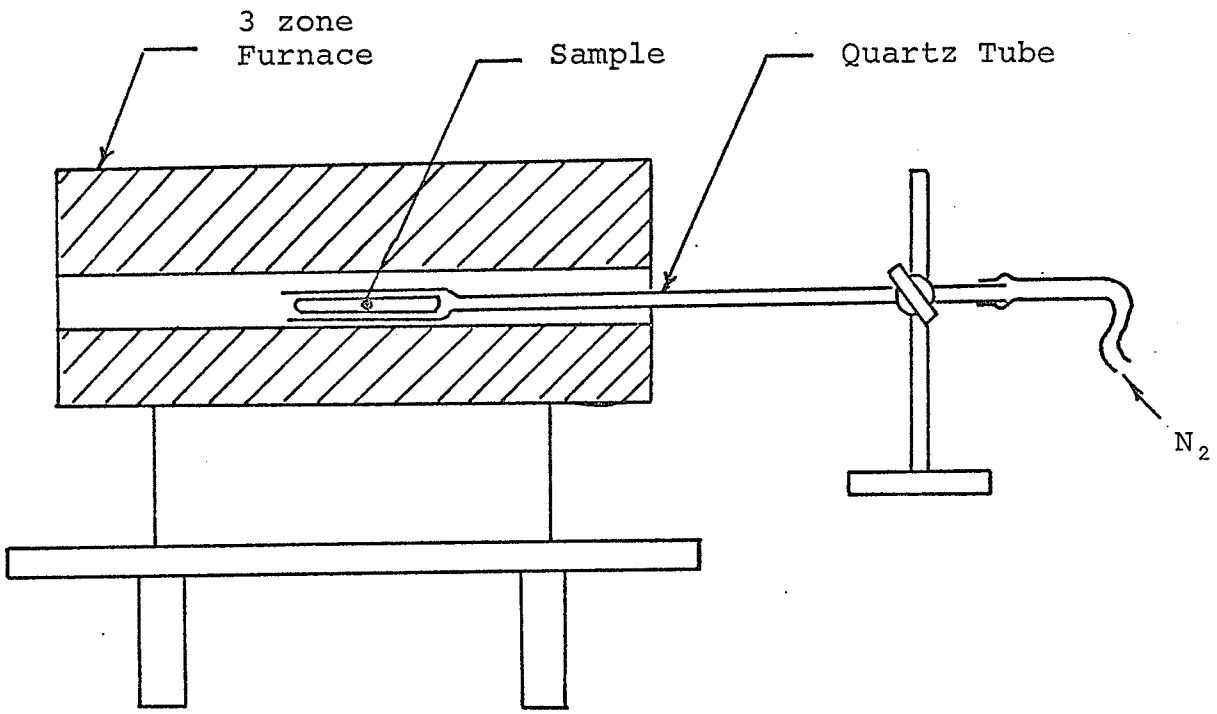

Fig. 4.1. Set-up for heat treatment of ohmic contacts.

4.2 The Sample Holder

The sample holder is made of a copper cylinder 2 inches in diameter and 4 inches in height, as shown in Fig. 4.2. The holder is fitted with a window to illuminate the sample. To avoid frosting at low temperatures, a double quartz window is used. To study the effect of the low temperatures the cylinder is immersed into a liquid nitrogen Dewar flask. For high temperature measurements a nichron heating coil is wound on a small insulated cylinder which is then placed axially inside the holder.

The sample is mounted on two tungsten electrodes inside an evacuated glass container. The temperature is measured using a copper constantan thermocouple. This design provides a high degree of temperature stability, and hence no temperature control system is needed.

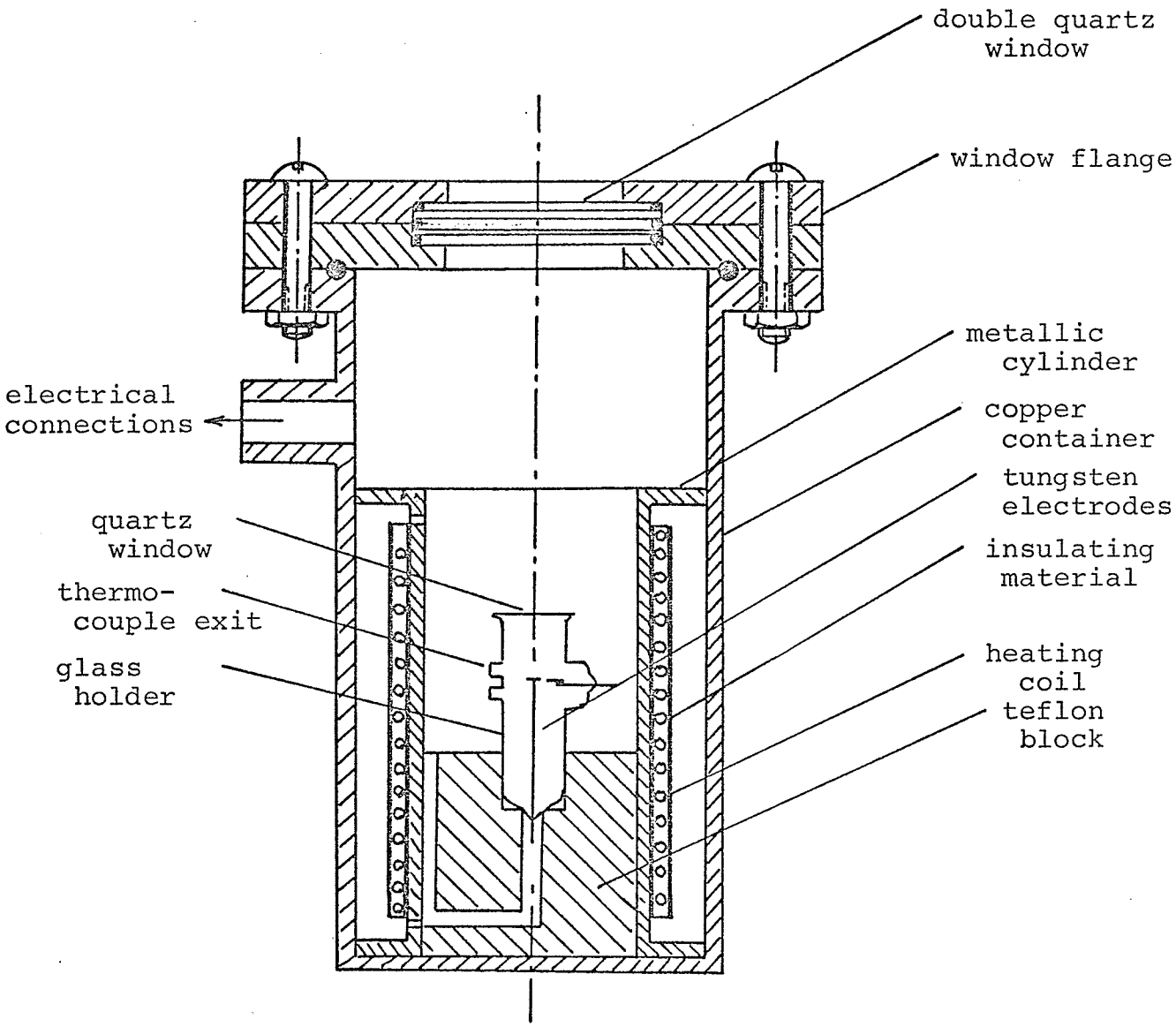

Fig. 4.2. Sample holder.

4.3 Experimental Procedure

4.3.1 Current-voltage Characteristics

The current-voltage characteristics of the sample at various temperatures are obtained by using a curve tracer (Tektronix Type 575). The experimental set-up is shown in Fig. 4.3. The sample holder is immersed in liquid nitrogen until the lowest temperature is reached, then current is passed through the heating coil to obtain various temperatures. Above room temperature only the heating coil was used. The current-voltage curves are taken every 25°K. To avoid Joule heating, which may disturb the lattice temperature, the curve tracer is switched on just before the required temperature is reached, and then quickly switched off after the oscillogram is photographed.

4.3.2 Oscillation Observation

The experimental set-up is shown in Fig. 4.4. Due to the fact that only small values of current are passing through the samples a d.c. current source can be used to bias the sample. However, biasing should not be applied for a long time to avoid heating up the sample. The biasing point must be on the n.d.r. region of the current-voltage characteristic obtained by the curve tracer. A voltmeter, as well as an ammeter are used to determine such a point. Temperature variation is carried on in the same way used for current-voltage tracing described in section 4.3.1. Oscillo-

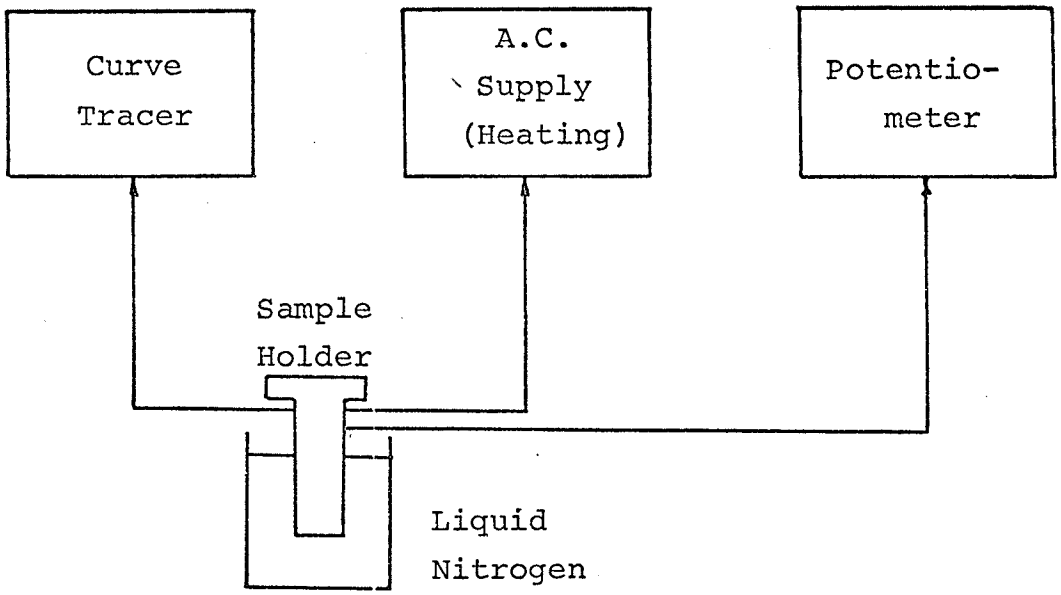

Fig. 4.3. Experimental Set-up (1) for current-voltage characteristic measurements.

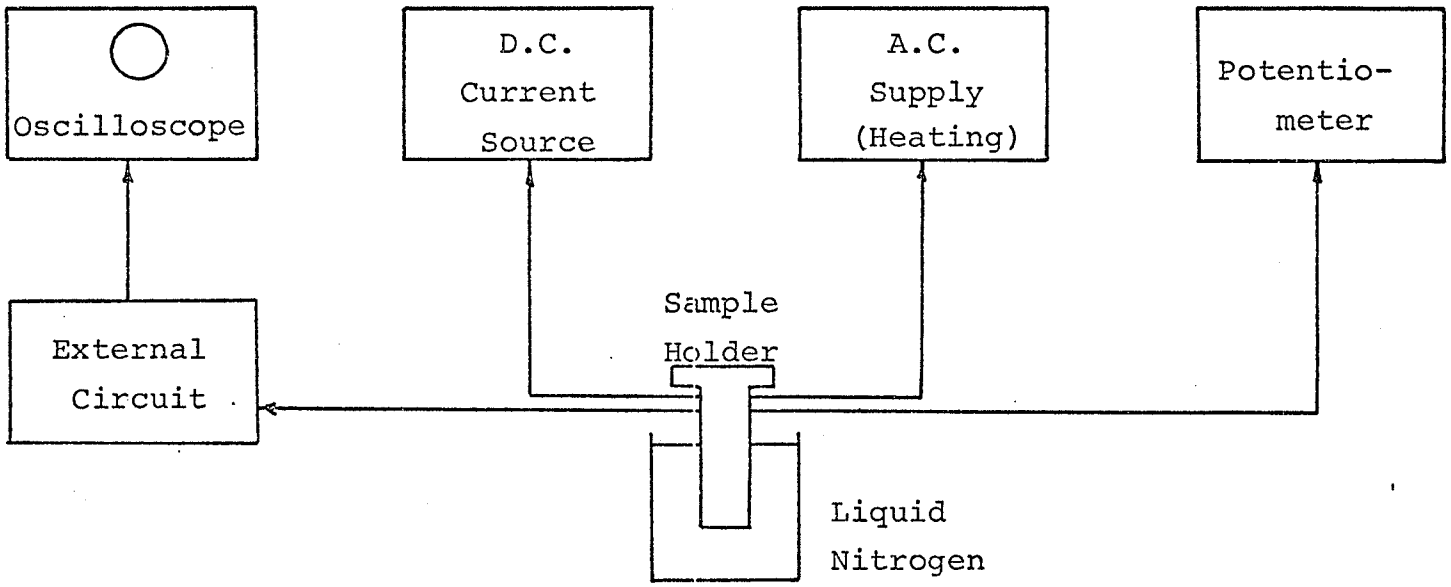

Fig. 4.4. Experimental Set-up (2) for current oscillation.

grams were photographed every 25°K. An external circuit similar to that used in tunnel diode oscillators is used, as shown in Fig. 4.5. A storage scope (Tektronix Type 549) is used to observe the oscillations.

4.3.3 Radiation Effects

In order to study the effect of radiation on n-type GaAs, a sample was irradiated in a gammacell 220, which is a cobalt 60 source with a half-life time of 5.27 years. The dose rate was measured with ferrous sulphate dosimetry. The dose rate at the time of the experiment was $0.5013 \times 1.6 \times 10^6$ rad/hr. The sample was irradiated every 10 minutes and the current-voltage characteristics were measured until no change was observed (saturation).

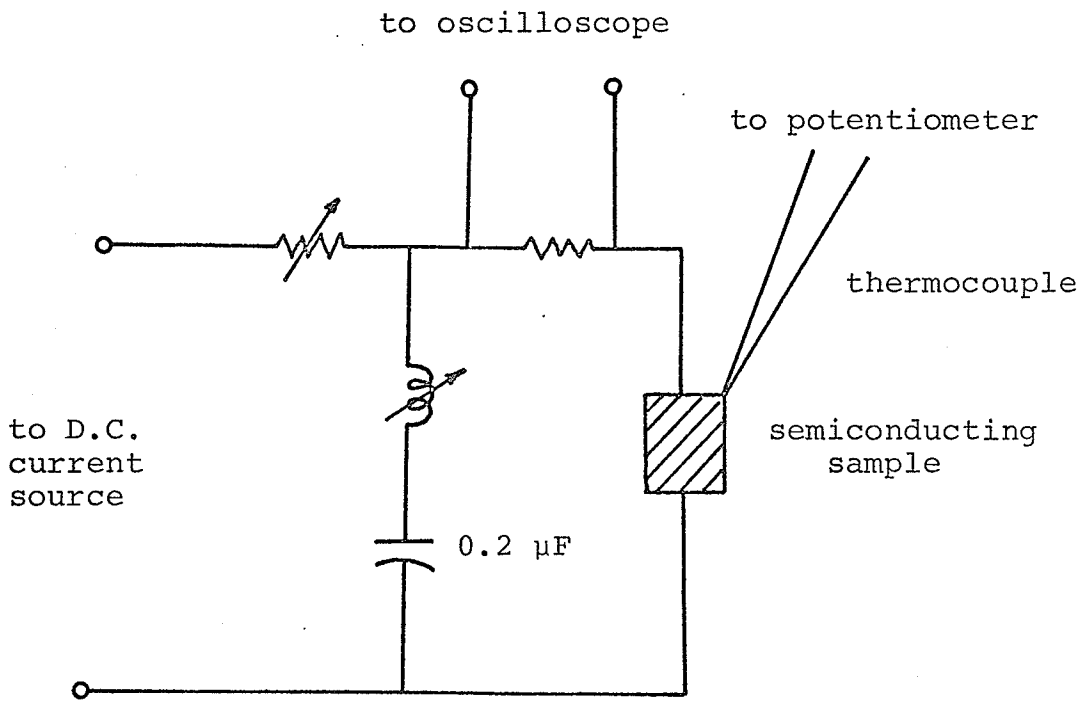

Fig. 4.5. External oscillating circuit.

CHAPTER 5

EXPERIMENTAL RESULTS AND DISCUSSION

5.1 Effects of Temperature on Current-voltage (I-V) Characteristics

The current-voltage characteristics were recorded by a curve tracer and the oscillograms are given in Fig. 5.1 - Fig. 5.4. The I-V characteristics are temperature dependent, and the negative differential resistance region appears at all temperatures except below -80°C, at and below which no n.d.r. could be observed. The threshold current for the onset of n.d.r. is practically independent of temperature, while the corresponding threshold voltage across the sample decreases with increasing temperature, as shown in Fig. 5.5. That the threshold current is independent of temperature may be explained as follows: As the temperature increases, the average energy of the free charge carriers increases, and consequently the possibility of surmounting the potential barrier before being captured by the recombination centers increases. But it is also possible that the barrier height ϕ (Fig. 3.1) may also increase with temperature owing to the temperature dependence of polarization of the surrounding atoms. This counteracts the increase of the average electron energy due

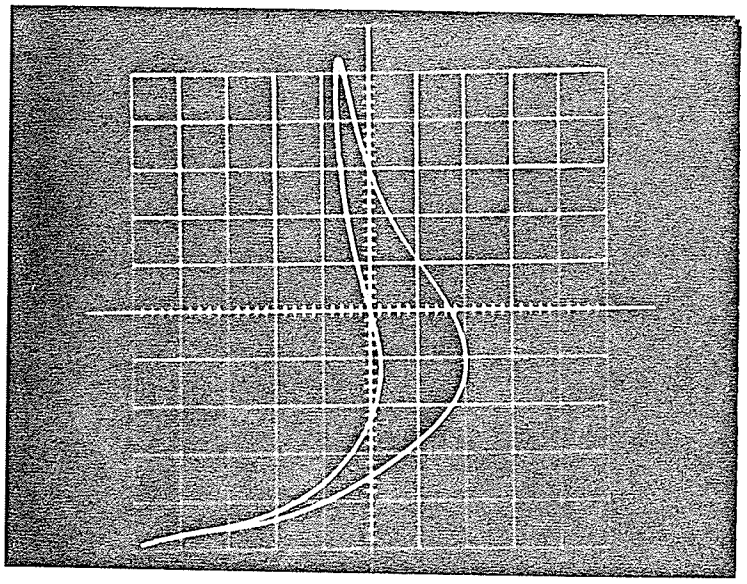

Fig. 5.1. I-V Characteristics at 88°C

Horizontal 5 v/div
Vertical 5 mA/div

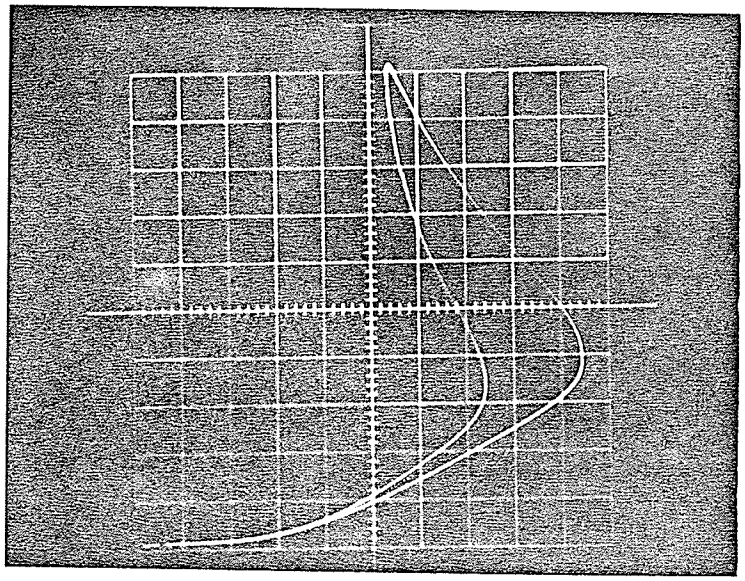

Fig. 5.2. I-V Characteristics at 21°C

Horizontal 5 v/div
Vertical 5 mA/div

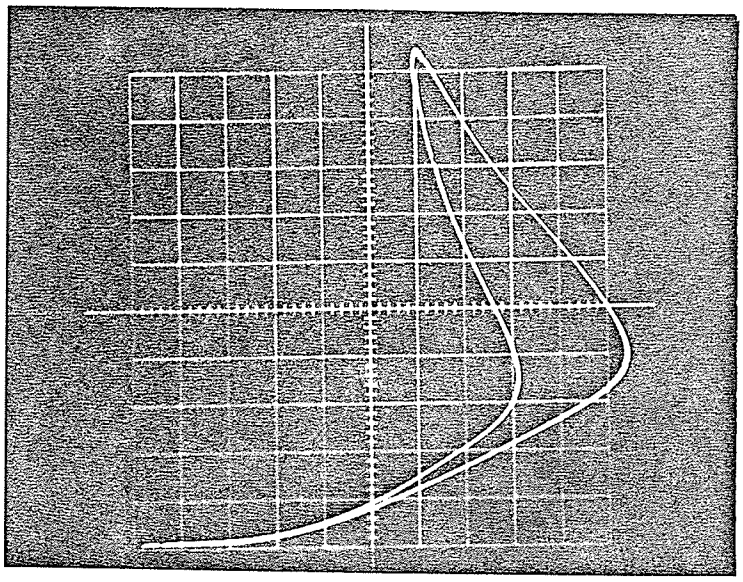

Fig. 5.3. I-V Characteristics at 0°C

Horizontal 5 v/div
Vertical 5 mA/div

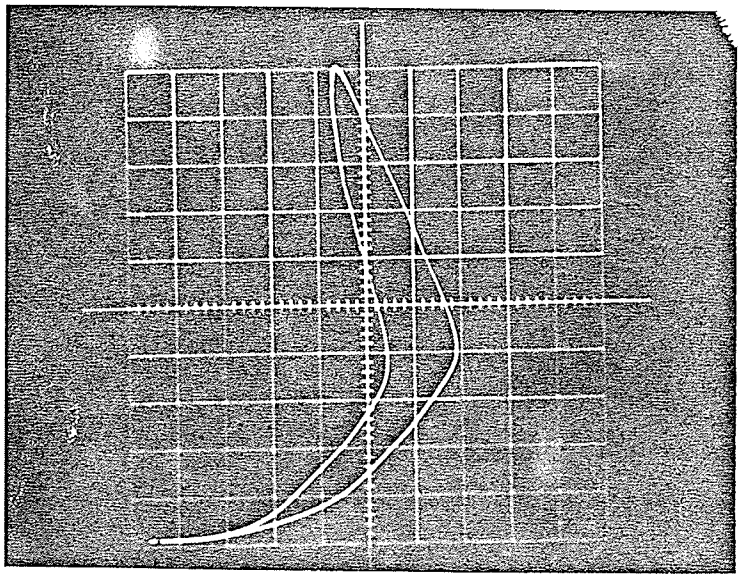

Fig. 5.4. I-V Characteristics at -75°C

Horizontal 10 v/div
Vertical 5 mA/div

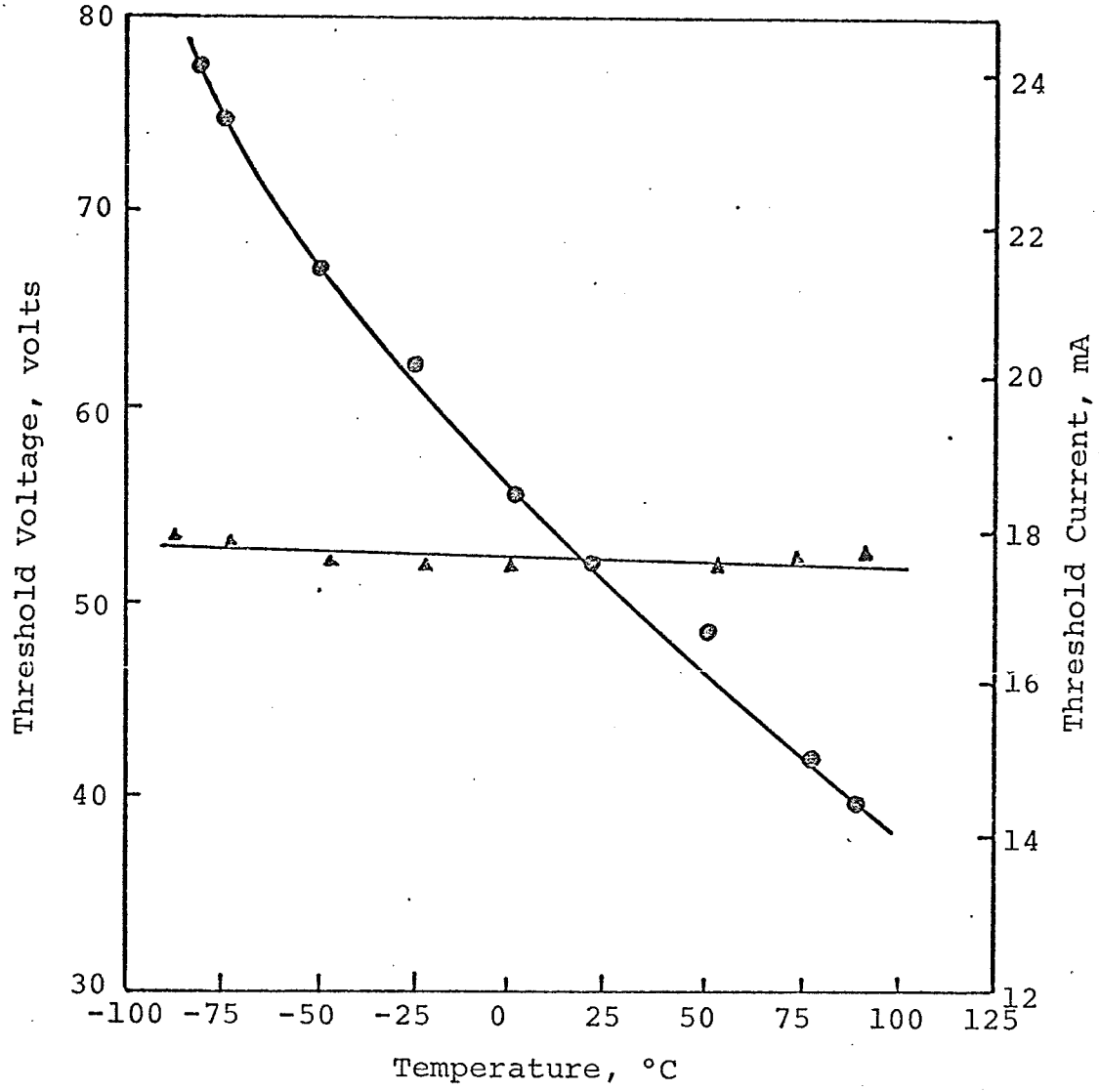

Fig. 5.5. Dependence of threshold voltage and current on temperature.

to the increase of temperature, and hence causes the threshold current to be independent of temperature. Since the number of carriers increases with temperature, the resistance and hence the voltage across the sample decreases when the temperature is increased as expected.

5.2 Effects of Temperature on Oscillation Amplitude and Frequency

The frequency of oscillation is temperature dependent despite the use of a predetermined tuned circuit, as shown in Figs. 5.6 and 5.7. It should be noted that the applied currents are different from each other due to the change of the negative differential resistance with temperature. The amplitude of oscillation decreases with increasing lattice temperature, whereas the frequency of oscillation increases with increasing temperature, as shown in Figs. 5.8 and 5.9. This temperature dependence of oscillation frequency can be explained as follows; since the storage time in the trapping center decreases with increasing temperature it would be expected that the higher the temperature, the shorter is the storage time, and consequently the higher is the frequency of oscillation. From Fig. 5.1 to Fig. 5.4 it becomes apparent that the higher the temperature, the shorter the length of the n.d.r. region due to the change of the number of free charge carriers and hence the smaller the amplitude of oscillation.

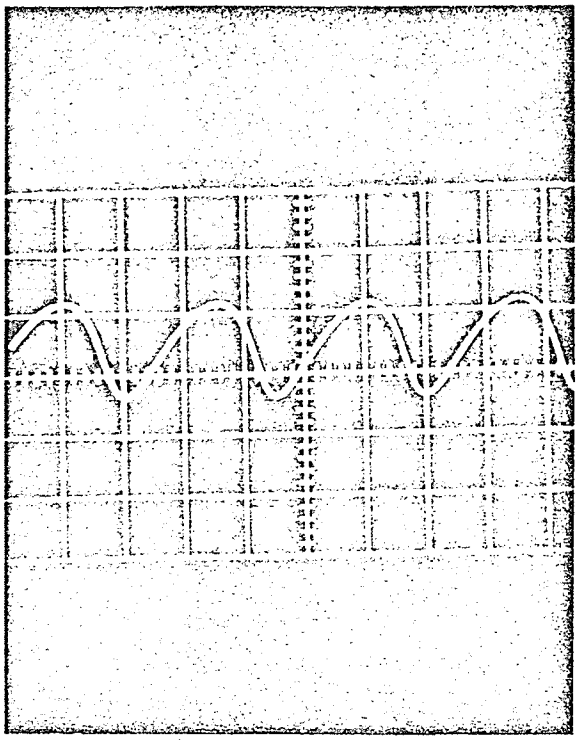

Fig. 5.6. Current Oscillations at -25°C

Horizontal 0.5 ms/div
Vertical 10 v/div

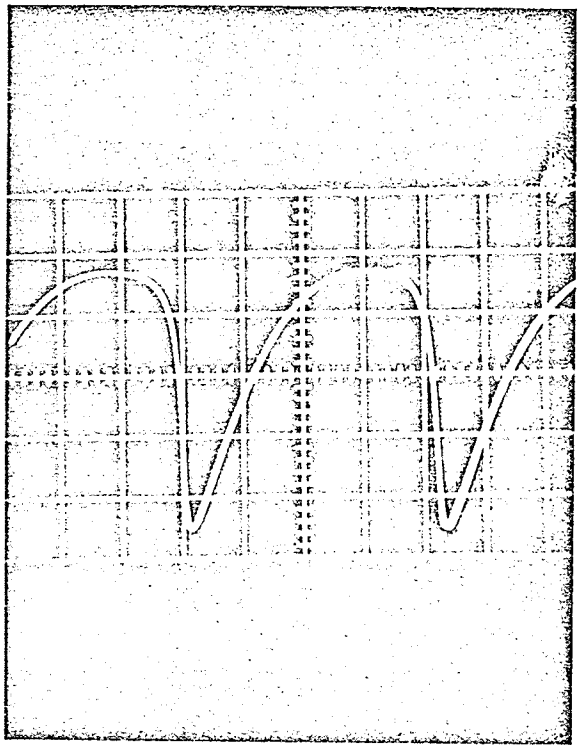

Fig. 5.7. Current Oscillations at -52°C

Horizontal 0.5 ms/div
Vertical 10 v/div

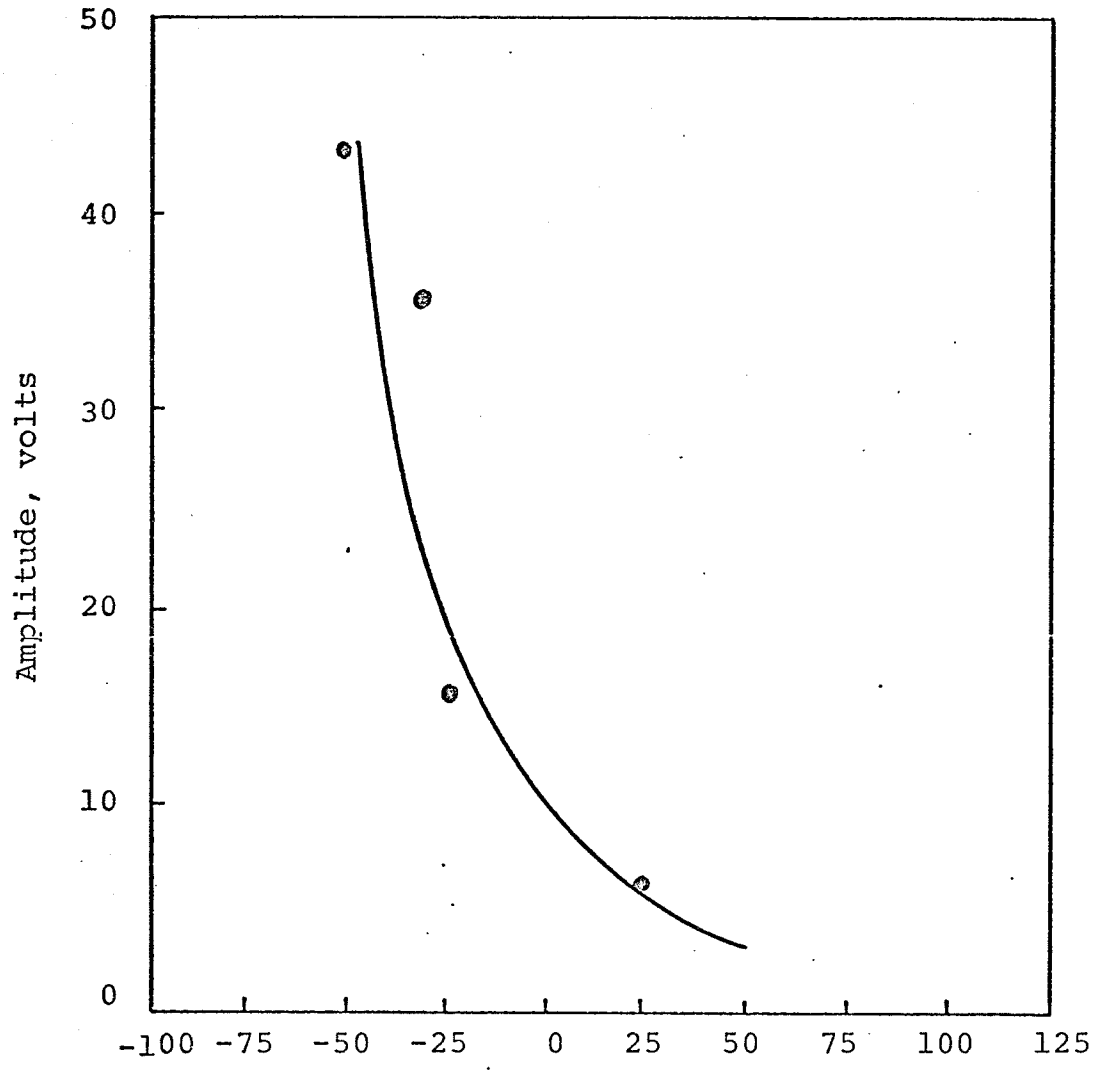

Fig. 5.8. Dependence of oscillation amplitude on temperature.

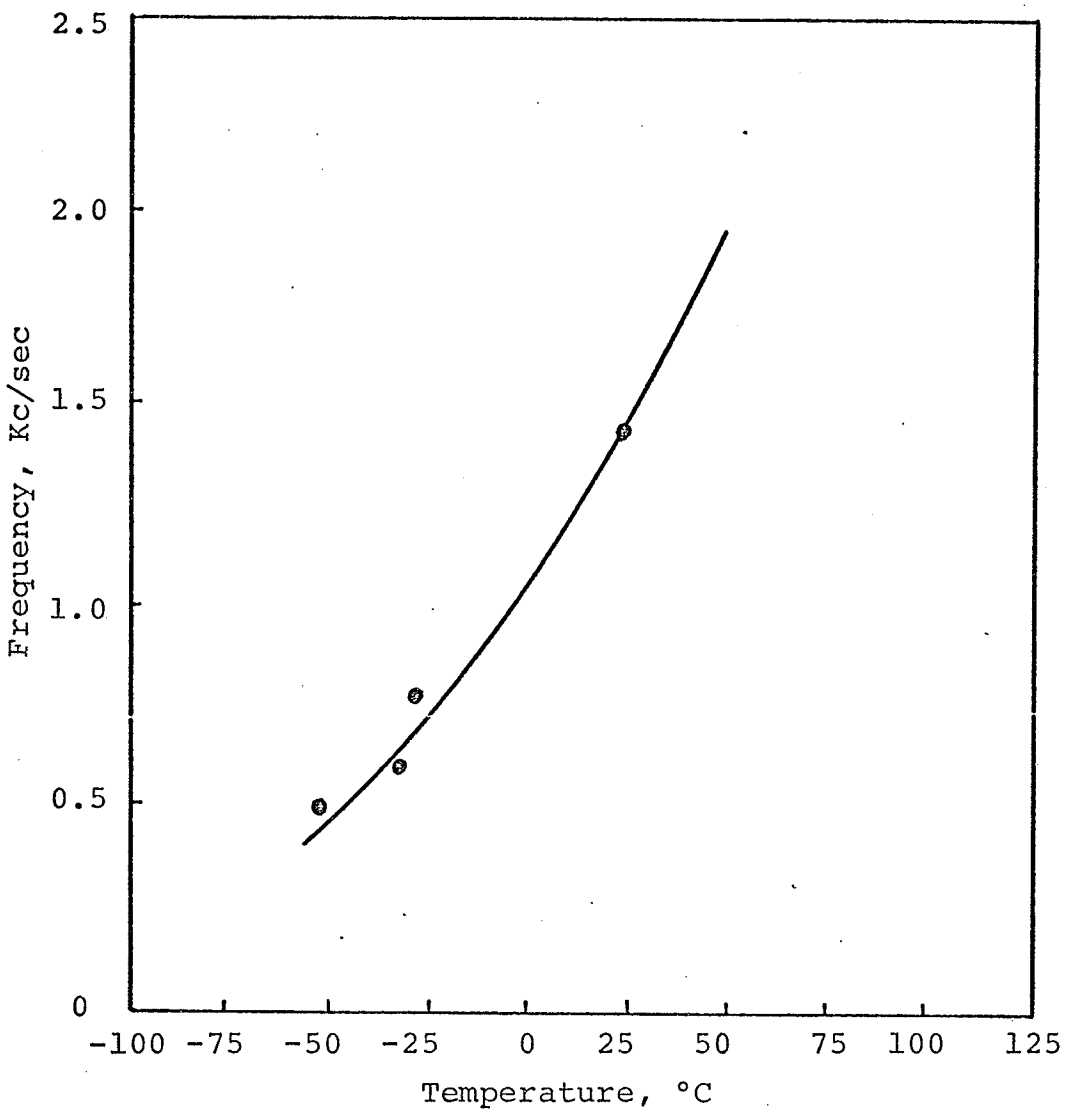

Fig. 5.9. Dependence of oscillation frequency on temperature.

5.3 Effects of Gamma Radiation

The current-voltage characteristics as functions of the gamma radiation dose are shown in Figs. 5.10 to 5.13. The total integrated time to reach saturation was approximately 2 hours, which corresponds to $2 \times 0.5013 \times 1.6 \times 10^6$ rads. The threshold current increases, while the corresponding voltage decreases with increasing radiation dose, as illustrated in Fig. 5.14 and Fig. 5.15.

The gamma radiation causes some atoms to displace from their lattice sites to interstitials in the semiconductor and therefore creates more trapping centers. These trapping centers may be quite different from those created by doping impurities. These centers capture electrons, thus reducing free electrons density, and therefore they would tend to modify the barrier and the probability of free electrons being captured by Coulombic recombination centers. Therefore, higher current is required to cause the onset of a negative differential resistance. On the other hand the increase in trapping centers tends to decrease the threshold voltage, as predicted by the theory.

The gamma radiation also affects the current oscillation, as shown in Figs. 5.16 and 5.17. Both the oscillation frequency and amplitude decrease after irradiation.

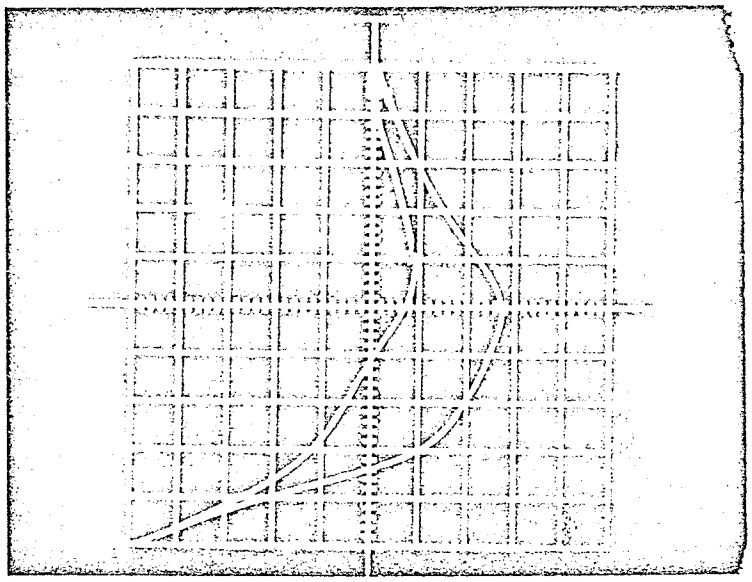

Fig. 5.10. I-V Characteristics, no radiation

Horizontal 5 v/div
Vertical 5 mA/div

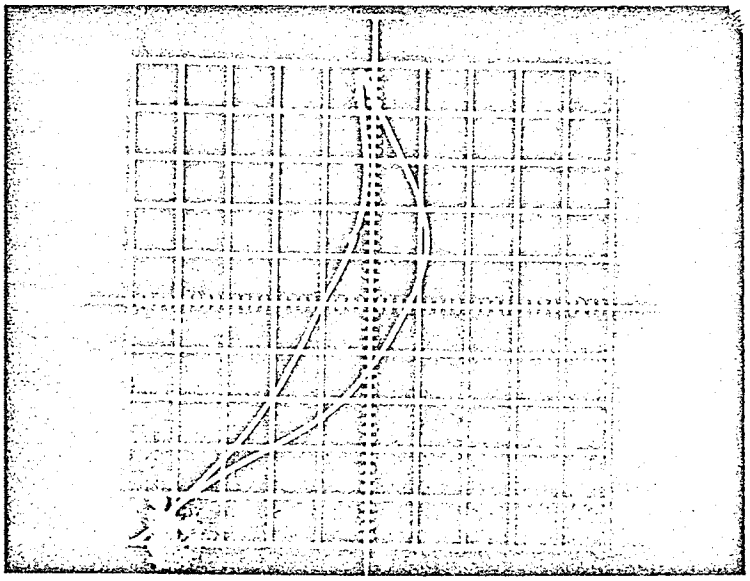

Fig. 5.11. I-V Characteristics, radiation dose = 0.8×10^6 rads

Horizontal 5 v/div
Vertical 5 mA/div

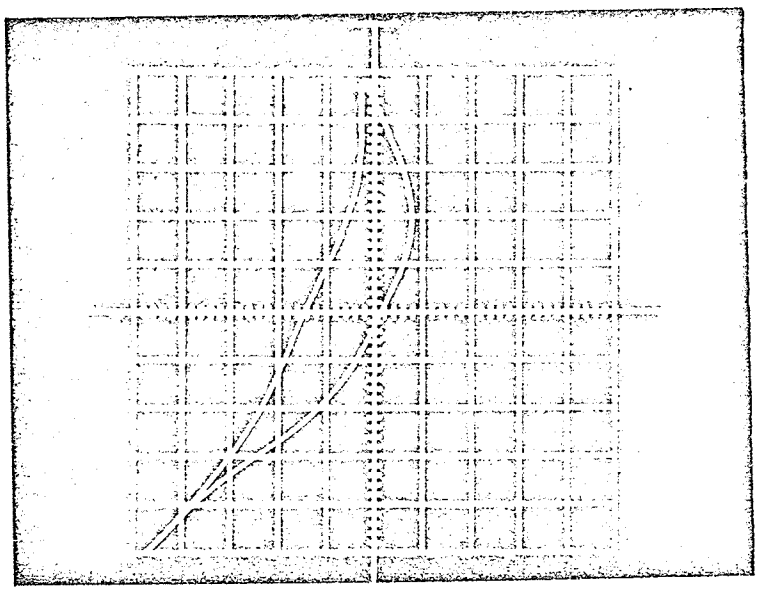

Fig. 5.12. I-V Characteristics, radiation dose = 1.6×10^6 rads.

Horizontal 5 v/div
Vertical 5 mA/div

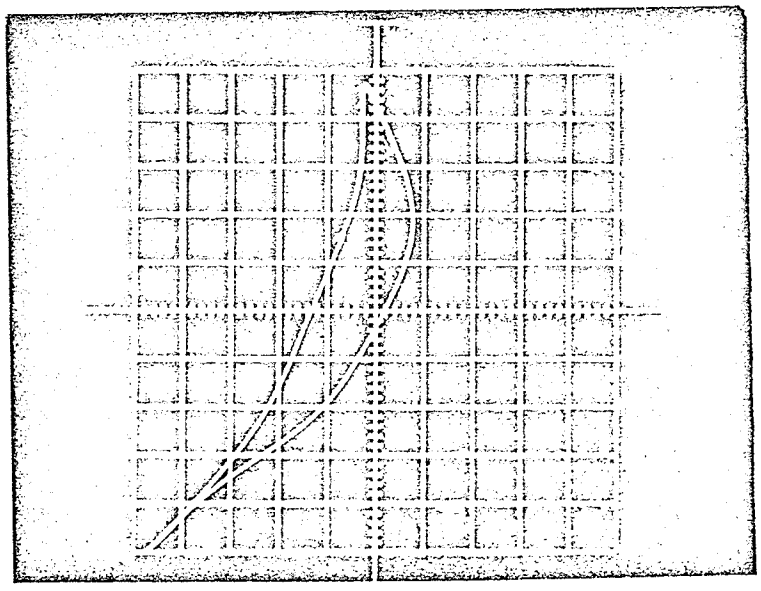

Fig. 5.13. I-V Characteristics, radiation dose = 2.4×10^6 rads.

Horizontal 5 v/div
Vertical 5 mA/div

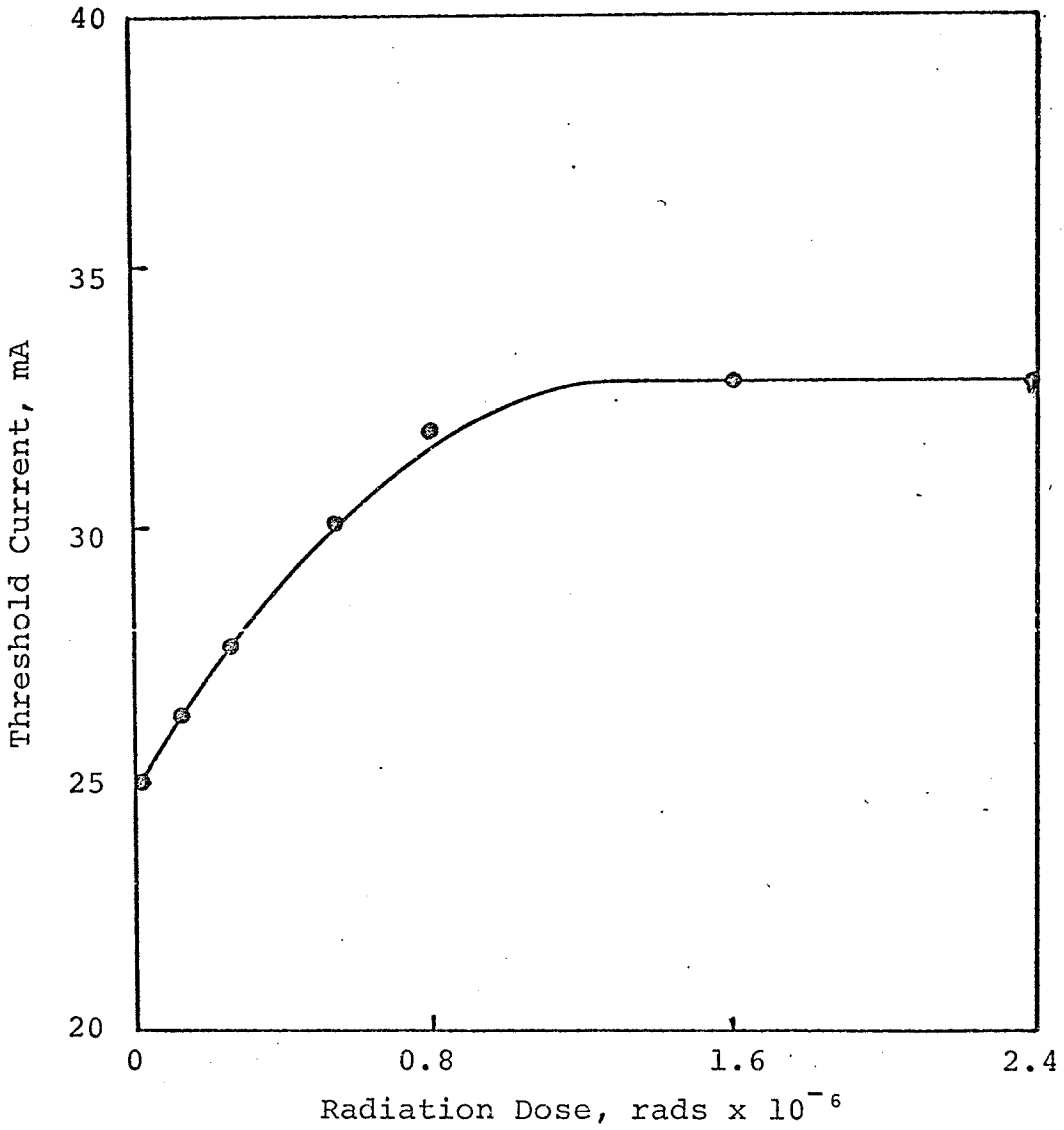

Fig. 5.14. Effect of gamma radiation on the threshold current.

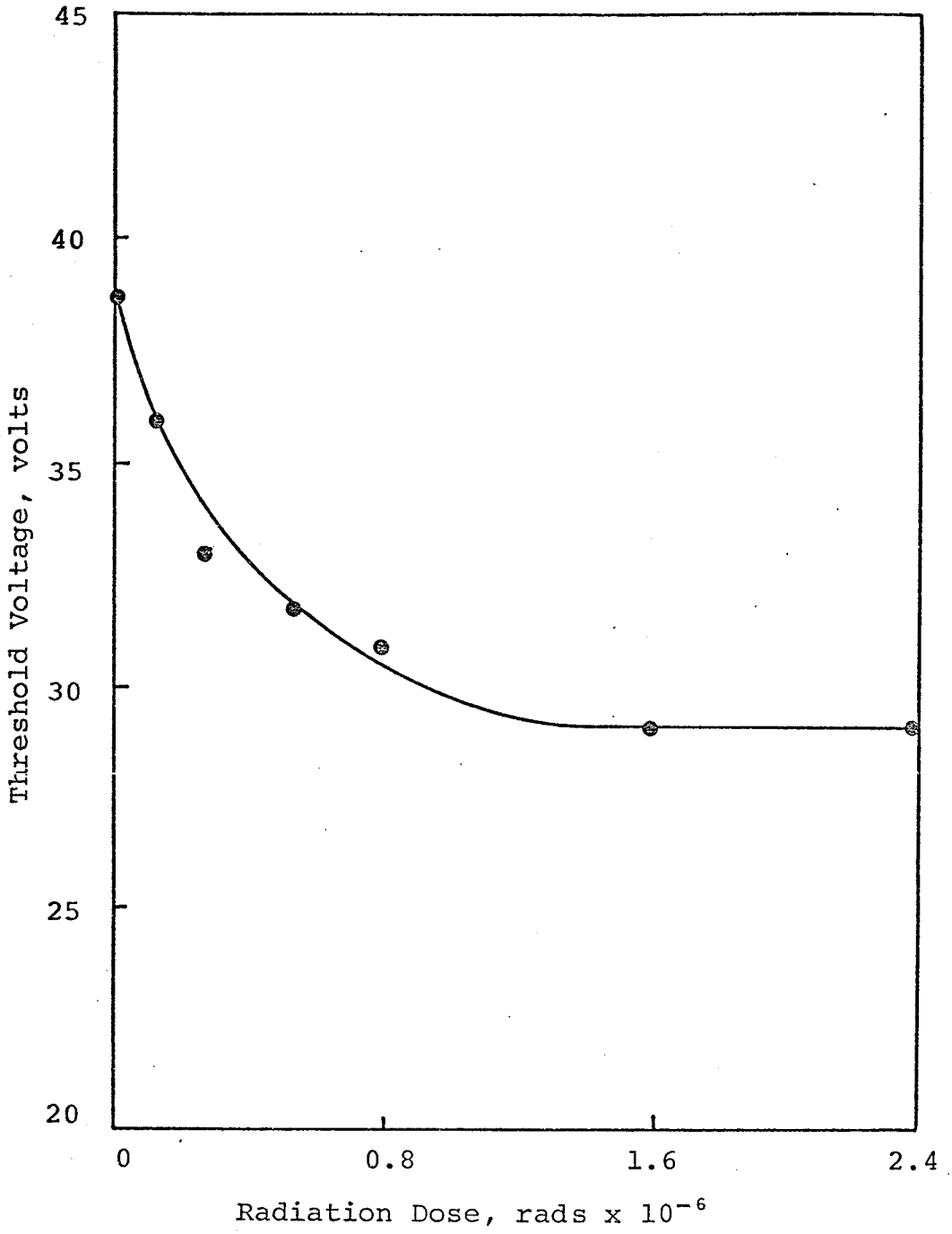

Fig. 5.15. Effect of gamma irradiation on the threshold voltage.

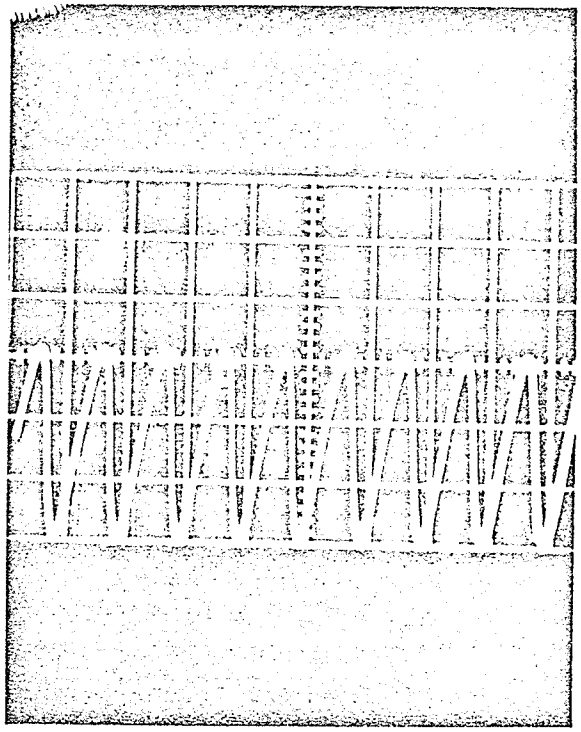

Fig. 5.16. Current Oscillations before irradiation

Horizontal 0.5 ms/div
Vertical 10 v/div

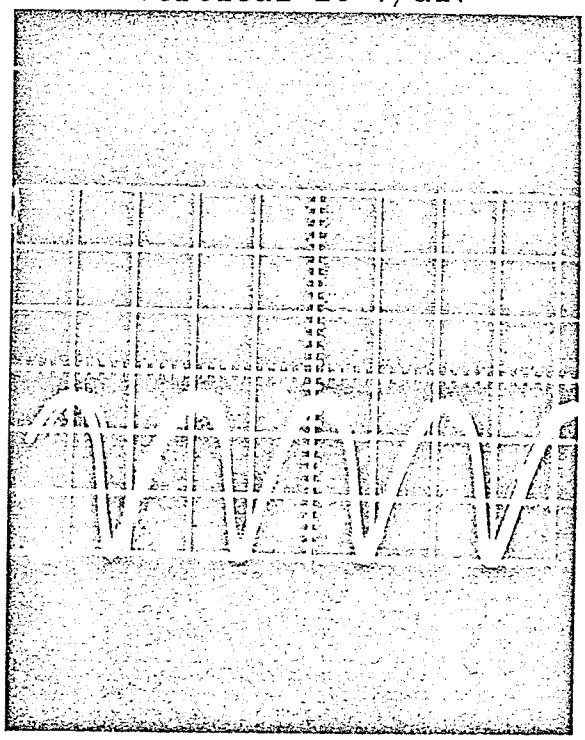

Fig. 5.17. Current Oscillations after irradiation with dose = 1.28 x 10^7 rads

Horizontal 0.5 ms/div
Vertical 10 v/div

5.4 Isochronal Annealing

After irradiation with a radiation dose of 1.28×10^7 rads, the isochronal annealing was then performed by increasing the temperature in 25°C steps with a period of 10 minutes of annealing at each step. As lead was used to mount the sample in a T0.5 header, the annealing temperature was limited to 325°C because the melting point of lead is 328°C.

The samples showed a tendency for recovery up to 275°C above which practically no change in the threshold voltage was observed, as shown in Fig. 5.18.

From Fig. 5.18, the threshold voltage increases as the annealing temperature increases. At temperatures near 125°C a steep decrease takes place and above this temperature it increases again until saturation is reached.

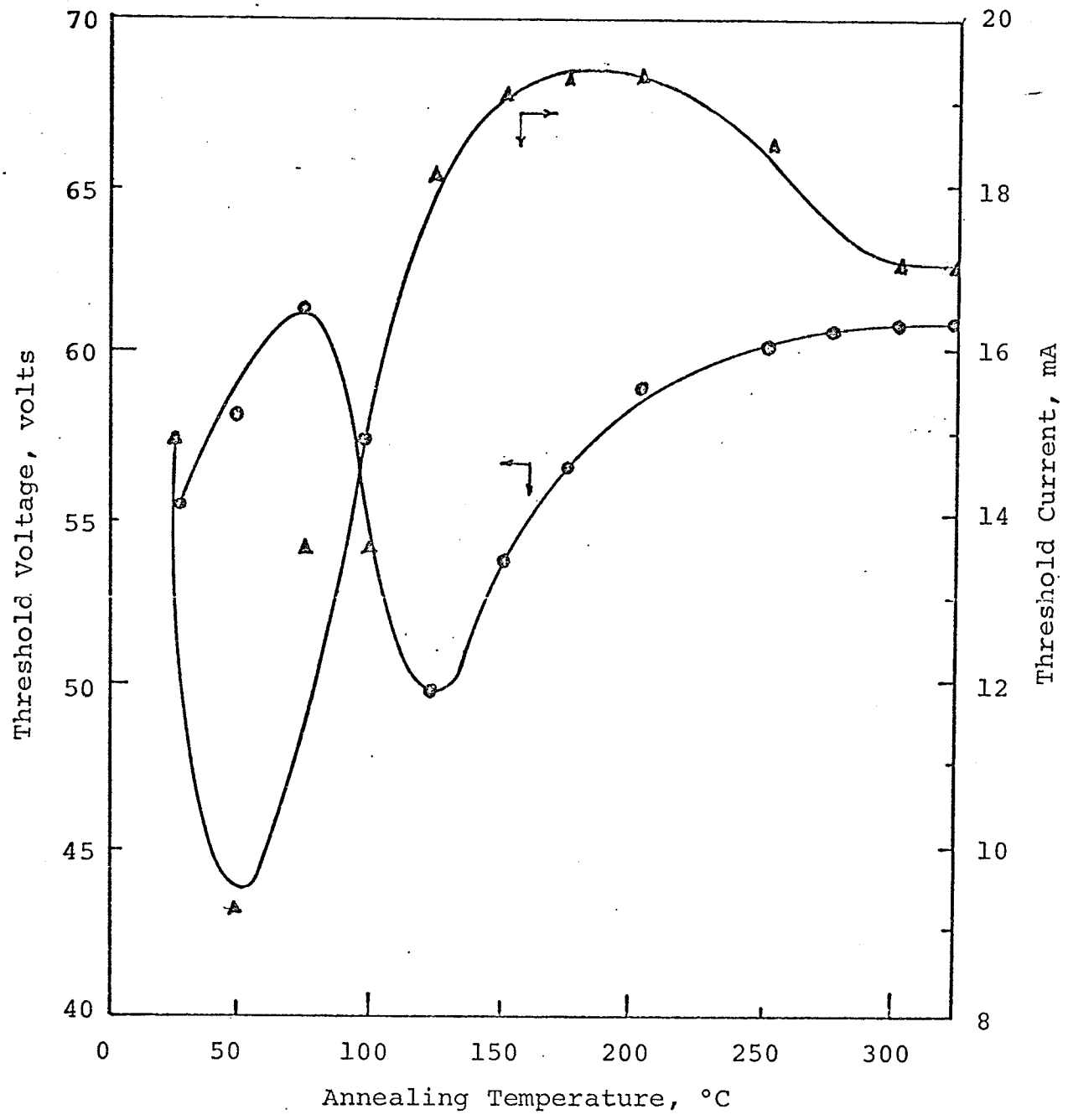

Fig. 5.18. Isochronal annealing of the threshold voltage and current.

CHAPTER 6

CONCLUSIONS

From the results described in Chapter 5 the following conclusions are drawn:

1. The current-voltage characteristics of n-type GaAs with high electron densities and the presence of Coulombic recombination centers, exhibit negative differential resistance regions of the S-shaped type.

2. The threshold voltage for the onset of n.d.r. decreases with increasing temperature, while the corresponding current is temperature independent.

3. Experimental results agree with the computed results obtained by considering the electron-electron scattering to be the dominant scattering mechanism.

4. Both the frequency and amplitude of the current oscillations in the n.d.r. region decreases with increasing temperature.

5. The threshold voltage decreases, whereas the threshold current increases with increasing gamma radiation dose. Both the oscillation frequency and amplitude decrease with increasing radiation dose.

6. The total integrated radiation dose to cause

the radiation effect to reach saturation is 2 x 1.6 x 0.5013 x 10^6 rads.

7. Isochronal annealing tends to recover the properties of the samples which have been changed due to gamma irradiation.

BIBLIOGRAPHY

Adawi, J., "Variational treatment of warm electrons in non-polar crystals," *Phys. Rev.*, 120, 120-127, 1960.

Adawi, J., "Negative resistance and hot electrons," *J. App. Phys.*, 32, No. 6, 1101-11, 1961.

Ando, K., Steele, M. C., and Lampert, M., "Negative resistance in constricted semiconductors," *J. Phys. Soc. Japan*, 18, No. 4, 591, 1963.

Ando, K., "A double injection negative resistance in p-type InSb at 77°K," *Jap. J. of App. Phys.*, 3, No. 12, 757-60, 1964.

Battey, J. F. and Baum, R. M., "Carrier capture probabilities in nickel doped germanium," *Phys. Rev.*, 100, 1634-37, 1955.

Bohm, J. and Farnell, G. W., "Low frequency instabilities in semi-insulator GaAs," *Proc. IEEE (Correspondence)*, 54, 890-91, 1966.

Bonch-Bruevich, V. L. and Kalashnikov, S. G., "The possibility of recombination instability in semiconductors," *Sov. Phys. Solid State*, 7, No. 3, 599-604, 1965.

Bonch-Bruevich, V. L., "Semiconductors and semimetals," *Physics of III-V Compounds*, 1, Acc. Press. N.Y., 1966.

Butcher, P. N., "The Gunn effect," *Rept. on Prog. in Phys.*, 30, part 1, 97-147, 1967.

Cleary, J. F., Editor, *G.E. Transistor Manual*, General Electric Company, 1964.

Cox, R. H. and Strack, H., "Ohmic contacts for GaAs devices," *Solid State Electronics*, 10, 1213-18, 1967.

Cunnell, F. A., Edmond, J. T., and Harding, W. R., "Technology of gallium arsenide," *Solid State Electronics*, 1, 97-106, 1960.

Dale, J. R. and Turner, R. G., "Simple ohmic contacts on gallium arsenide," *Solid State Electronics*, 6, 388-90, 1963.

Day, G. F., "Two bulk negative resistance effects in high

resistivity GaAs," *Bull. Am. Phys. Soc. (Sec. 2)*, 10, 383, 1965.

Dorman, P. W., "Domain properties in GaAs oscillating at KHz frequencies," *Proc. of the IEEE*, 56, No. 3, 372-73, 1968.

Ehrenreich, H., "Band structure and electron transport of GaAs," *Phys. Rev.*, 120, No. 6, 1951-63, 1960.

Foyt, A. G., Jr., "Gunn effect in compound semiconductors," Technical Report, Lincoln Laboratories, MIT, 1965.

Frölich, H. and Paranjape, B. V., "Dielectric breakdown in solids," *Proc. Phys. Soc.*, B 69, 21-32, 1956.

Gaylord, T. K., Shah, P. L., and Rabson, T. A., "Gunn effect bibliography," *IEEE Trans. Electron Devices*, ED-15, No. 10, 777-88, 1968.

Gaylord, T. K., Shah, P. L., and Rabson, T. A., "Gunn effect bibliography supplement," *IEEE Trans. Electron Devices*, ED-16, No. 5, 490-94, 1969.

Gunn, J. B., "Microwave oscillations of current in III-V semiconductors," *Solid State Com.*, 1, 88-91, 1963.

Gunn, J. B., "Instabilities of current in III-V semiconductors," *I.B.M. J. Res. Dev.*, 8, 141, 159, 1964.

Hilsum, C., "Transferred electron amplifiers and oscillators," *Proc. IRE*, 50, 185-89, 1962.

Hughes, W. E., "Current controlled negative resistance in n-type Gallium Arsenide," *Proc. IEEE (Letters)*, 56, 1715, 1968.

Johanson, L. and Levinstien, H., "Infrared properties of gold in germanium," *Phys. Rev.*, 117, 1191, 1960.

Kikuchi, M., "Experimental observation of travelling high electric field domain in oxygen-doped GaAs," *Solid State Com.*, 5, 855-858, 1967.

Landau, L. D. and Lifshitz, E. M., *Statistical Physics*, Addison-Wesley Pub. Company Inc., Reading, Mass., 268, 1958.

Law, H. C. and Kao, K. C., "Current oscillations caused by recombination centers in semiconductors," *Solid State Electronics*, 13, 659-69, 1969.

Matsumo, K., "Low frequency current fluctuations in GaAs Gunn diode," *App. Phys. Letters*, 12, No. 12, 404-05, 1968.

Mizushima, Y., Igarashi, Y., and Ochi, O., "Switching characteristics of the GaAs films," *Proc. IEEE (Correspondence)*, 53, 322-23, 1965.

Oliver, D. J., "Electrical properties of n-type GaAs," *Phys. Rev.*, 27, No. 4, 1045-52, 1962.

Pamplin, B. R., "Negative differential conductivity effects in semiconductors," *Contemp. Phys.*, 11, No. 1, 1-19, 1970.

Phelan, R. J. and Love, W. F., "Negative resistance and impact ionization impurities in n-type InSb," *Phys. Rev.*, 13, No. 4A, A1134-37, 1964.

Ridley, B. K. and Watkins, T. B., "The possibility of negative resistance effects in semiconductors," *Proc. Phys. Soc.*, London, 78, 293-303, 1961.

Ridley, B. K. and Watkins, T. B., "Negative resistance and high electric field capture rates in semiconductors," *J. Phys. Chem. Solids*, 22, 155-58, 1961.

Ridley, B. K. and Pratt, R. G., "A bulk differential negative resistance due to electron tunnelling through an impurity potential barrier," *Phys. Letters*, 4, No. 5, 300-02, 1963.

Ridley, B. K. and Pratt, R. G., "Hot electrons and negative resistance at 20°K in n-type germanium containing Au^{--} centers," *J. Phys. Chem. Solids*, 26, 21-31, 1965.

Ridley, B. K. and Wisbey, P. H., "Hot electron capture at platinum centers in n-type germanium," *J. Phys. C: Solid State Phys.*, 3, 211-21, 1970.

Shirafuji, J., "Current oscillations and some photo-electric properties in high resistivity GaAs produced by irradiation of fast neutrons," *Jap. J. App. Phys.*, 8, No. 7, 898-909, 1969.

Shulman R. G. and Wyluda, B. J., "Cu in Ge: Recombination center and trapping center," *Phys. Rev.*, 102, 1455-57, 1956.

Spenke, E., *Electronic Semiconductors*, McGraw Hill Book Comp., Inc., N.Y., 45, 1958.

Straton, R., "The influence of interelectronic collisions on conduction and breakdown in polar crystals," *Proc. Roy. Soc.*, 246A, 406-22, 1958.

Sugiyama, K., "Recombination and trapping processes at deep centers in n-type GaAs," *Jap. J. App. Phys.*, 6, No. 5, 601-11, 1967.

Tokumaru, Y., "Current oscillations by two bulk negative resistance effects in photoexcited GaAs," *App. Phys. Letters*, 14, No. 7, 212-13, 1969.

Wu, S. M., "Microwave complex permittivities of Si and GaAs at high electric fields, and Gunn instabilities at various temperatures and magnetic fields," M.Sc. Thesis, University of Manitoba, Canada, May, 1970.

Yamashita, J., "Electron-electron interaction in hot electron problems," *Prog. Theort. Phys. (Kyoto)*, 24, 357-69, 1960.

Yamamoto, R., "Current Oscillation in CaS", *Jap. J. App. Phys.*, 5, No. 5, 351-57, 1966.